

## MODELLING OF MUSCLE INFLUENCE ON THE KINEMATICS OF THE HEAD-NECK COMPLEX IN IMPACTS

Adam WITTEK and Janusz KAJZER

*Department of Mechanical Engineering, Nagoya University*

(Received October 27, 1997)

### Abstract

The purpose of the present study is to perform mathematical modelling analysis of muscle effect on the kinematics of the human body in a car collision. The study is divided in two parts: 1) Multibody analysis of muscle effect on response of the human head-neck complex in a frontal car collision and 2) Development of finite element Hill-type muscle model for investigation of muscle effect on the biodynamic response of the human body to transient loads.

The parameter study of muscle effect in a frontal car collision was done to analyse two important problems: 1) Influence of the triggering times of the muscle activity on the head-neck complex response, and 2) Sensitivity of the calculated muscle effect to parameters and structure of the muscle model. In order to investigate these two problems, a simplified multibody model of the head-neck complex, with the neck treated as a single rigid link, was used. Results obtained with this model indicated that muscles can significantly affect kinematics of the head-neck complex in frontal impacts only when the horizontal acceleration of a car during a crash is not greater than 15 g, and when the reflex time is lower than 60 (80) ms. Furthermore analysis of these results suggested that complexity and determining the parameters of the Hill-type muscle model are not the crucial points in the investigation of the muscle effect on the biodynamic response of the head-neck complex in a car collision. Differences between various kinds of the Hill-type models were not strong enough to significantly affect structural response of the model of the head-neck complex. The validity of the simplified model of the head-neck complex was limited to the analysis of the muscle effect on the basic kinematics of the head-neck complex in frontal car collisions. It was deficient for in more detail investigation of muscle effect on the cervical spine kinematics and the neck injuries.

Finite element analysis is a direct method to develop a head-neck model which enables such investigation. However, commercial finite element codes do not facilitate appropriate modelling of skeletal muscles. Thus, the authors

attempted to develop a new Hill-type model of skeletal muscle in finite element code PAM-CRASH, which is described in the second part of the present report. Results obtained with the current one-dimensional muscle model indicated that this model is suitable for modelling essential features of skeletal muscle behaviour under both isometric contraction and transient load conditions. Therefore this model can be used as the basis for further development of two- and three-dimensional muscle models which are recommended for in-depth analysis of muscle effect on responses of the human body in car collisions.

**Keywords:** frontal car collision, head-neck complex kinematics, muscle effect, Hill-type muscle models, mathematical model, multibody model, finite element muscle model.

## Contents

Chapter 1. Parameter Study of Muscle Effect on Response of the Head-Neck Complex in a Frontal Car Collision .....	157
1.1 Introduction .....	157
1.2 Methods .....	159
1.2.1 Models .....	159
Head-neck model .....	159
Reflex time and neural control .....	162
Muscle models .....	163
Impact pulses .....	164
Programming and numerical methods .....	164
1.2.2 Parameter study of muscle influence .....	165
Influence of muscles at different impact severity and for different reflex time .....	165
Influence of reflex time and initial muscle tension .....	165
Influence of structure and parameters of muscle models .....	166
Influence of static neck strength .....	167
Test matrix .....	167
Head-neck model validation .....	167
1.3 Results .....	168
1.3.1 Influence of muscles at different impact severity and for different reflex time .....	168
Influence of reflex time and initial muscle tension .....	169
Influence of structure and parameters of muscle models .....	170
Influence of static neck strength .....	175
Results of validation .....	175
1.4 Discussion .....	176
Chapter 2. Development of a Hill-type Finite Element Muscle Model for Investigation of the Human Body Response Under Transient Load .....	178
2.1 Introduction .....	178
2.2 Methods .....	179
2.2.1 Mathematical formulae for Hill-type finite element muscle model .....	179
Formulae for contractile element .....	180
Formulae for parallel element .....	182
Formulae for series elastic element/tendon .....	183
Neural control and reflex time .....	184
Equilibrium of muscle-tendon unit .....	185

2.2.2 Software implementation of finite element muscle model .....	185
2.2.3 Model validation .....	186
2.3 Results .....	189
2.4 Discussion .....	192
Summary .....	196
Acknowledgements .....	196
Appendix 1: Dynamics of the head-neck model .....	197
Appendix 2: Dynamics of the muscle models .....	198
References .....	202

## **Chapter 1. Parameter Study of Muscle Effect on Response of the Head-Neck Complex in a Frontal Car Collision**

### **1.1 Introduction**

The role of muscles is seldom taken into account in analysis of the mechanisms of injuries to the neck in car crashes. Since the experimental literature has indicated that muscles can affect kinematics and kinetics of the head-neck complex when impact severity is not extremely high, disregarding the muscles may not always be appropriate. Important limitation of the literature data is that muscle activity during impacts still remains largely unquantified.

For instance, in the studies by Mertz and Patrick (1967, 1971) only two distinct physiological muscle states were distinguished: relaxed and tensed. Muscle tension was only roughly controlled; the subject was simply asked either to relax or to contract muscles. Mertz and Patrick (1967, 1971) analysed rear-end impacts with acceleration up to 6.6 g and speed up to 37 km/h. They found significant differences in the head kinematics and the maximum torques about the occipital condyles between a human subject with relaxed muscles, a human subject with tensed muscles, and cadavers, see Table 1. Important limitation of the studies by Mertz and Patrick (1967, 1971) is that only one 50th percentile human subject was used. Thus, generalisation of their results may not be appropriate.

Differences between cadaver and volunteer responses in frontal impacts have been also reported by Wismans *et al.* (1987). They found that in a 15 g impact, the peak angle of the head flexion in cadaver tests is greater than that in volunteer tests. One explanation could be that muscle tension restrains the motion of the head in volunteers. However, the muscle tension was not measured in the study by Wismans *et al.* (1987).

Muscle tension was more accurately controlled in the study by Verriest *et al.* (1972), who investigated the response of head-neck complex of baboons in frontal impacts. Subjects were anaesthetised to keep muscles in relaxed state, and electric stimulation was used to activate muscles. The results by Verriest *et al.* (1972) indicated that muscle tension can reduce maximum angular acceleration of the head by about 40% in frontal impact with acceleration of 20 g.

Bosio and Bowman (1986) observed phenomena which indirectly confirm that muscles can significantly influence the flexion/extension angle of the head in a car crash. They identified two modes of the head extension about the occipital condyles in frontal impacts: 1) extension with rebounding after reaching a given peak of extension angle, and 2) extension without rebounding after the first peak. The extension without rebounding can be related to significant activity of the neck extensors.

Potential relevancy of the muscle activity to analysis of the kinematics of the human head-neck complex in a low speed impact has been also discussed by Szabo and Welcher

(1996). They measured electromyographic signal from the human neck and lumbar muscles in rear impacts at a speed up to 14 km/h and acceleration up to 5 g. The electromyographic signal was obtained with surface electrodes. Szabo and Welcher (1996) measured that muscle activity occurs 100–125 ms after the moment of contact of a car bumper. They hypothesised that muscles may be triggered by centrally generated response. In the experiments by Szabo and Welcher (1996), all subjects kept muscles in relaxed state prior to impact. Therefore direct evaluation of the muscle effect is not possible with their data.

**Table 1** Summary of the results by Mertz and Patrick (1967, 1971)

Subject	Impact Severity	Max. Torque About Occipital Condyles	Max. Head Angle	Muscle Tension
Cadaver	16 km/h	20.3–37.5 Nm	No data	—
Human	16 km/h	16.7 Nm	No data	Tensed
Human	4.1 g	20.4 Nm	47°	Relaxed
Human	4.1 g	16.7 Nm	22°	Tensed

Better evaluation of muscle role in impacts requires information about muscle force. However, direct measurement of muscle force in volunteers under load of a car crash is strongly limited by ethical and technical reasons. Alternative solution is to use mathematical modelling to calculate muscle force. Muscle force can be predicted with various kinds of muscle models, such as purely phenomenological models which treat muscle as dynamic system of given order (Dabrowska and Kedzior, 1985; Kedzior and Lackowski, 1992), Hill-type models (Hill, 1938; Hatze 1981), cross-bridge model (Huxley and Hanson, 1954; Huxley 1969; Huxley, 1971), distribution-moment model (Zahalak, 1986; Zahalak and Ma, 1990; Ma and Zahalak, 1991) and models based on continuum mechanics (Huyghe *et al.*, 1991a; Huyghe *et al.*, 1991b; Taber, 1991a; Taber, 1991b; Fung, 1993). Cross-bridge model, distribution-moment model, and models based on continuum mechanics are far more complex than Hill-type models. For this reason the Hill-type models have been commonly used in impact biomechanics, *e.g.* study of the kinematics of the human cervical spine by Pontius and Liu (1976), and analysis of muscle effect on the kinematics of the head-neck complex by Happee and Thunnissen (1994a; 1994b).

The model of muscle by Happee and Thunnissen (1994a; 1994b) contains muscle mass, which makes it possible to investigate simultaneously two important aspects of muscle influence on the biodynamic response of the human body: 1) Influence of the muscle force, and 2) Influence of the muscle mass. Happee and Thunnissen (1994b) implemented their muscle model in a simplified mathematical model of the head-neck complex. With these models they estimated that muscles can reduce the maximum angle of head flexion by up to 50% in a frontal impact at a speed of 50 km/h and peak acceleration of 15 g.

In summary, several mathematical modelling studies have indicated that muscles can significantly decrease maximum flexion angle and maximum angular acceleration of the head, even in relatively severe impacts. However, four important aspects of muscle influence on the head-neck complex kinematics in impacts have not been explained enough in neither experimental nor mathematical modelling studies. The first aspect is that it has not been assessed at what level of impact severity the muscle effect becomes negligible. The second

aspect is that the knowledge how the nervous system controls the muscles in a car crash remains unclear. So far the stretch and visual reflexes have been the main consideration in the literature (Pontius and Liu, 1976; Happee and Thunnissen, 1994a). On the other hand, Szabo and Welcher (1996) found that the neck flexors and extensors exhibit similar onset times of the muscle activity in rear impacts. It corresponds to the centrally generated response rather than to the stretch reflex. The third aspect is that the muscle can be modelled in many different ways. There is no unique "standard" structure of a muscle model. The current study is focused on two kinds of models: 1) Hill-type models, and 2) A purely phenomenological model which assumes that muscle is a dynamic system of given order. Furthermore, the original concept by Hill (1938) is a lumped parameter model, which does not have direct connection with a real muscle structure. The elements of such a model can be identified with elements of muscle in many different ways, which results in various structures of Hill-type muscle models (Hatze, 1981; Winters and Stark, 1985; Pandey *et al.*, 1990; Winters, 1990; Giat *et al.* 1994; Happee and Thunnissen, 1994a). So far the sensitivity of the overall response of models of the human body segments to the structure of muscle models has not been analysed in impact biomechanics. However, studies of daily-life and sports activities have indicated that the results of modelling of musculoskeletal motion are sensitive to the complexity of the muscle model (Audu and Davy, 1985). The fourth aspect is that the muscle effect varies between individuals because of differences in strength of the neck muscles.

The present study is an attempt to analyse in more detail these four aspects of the muscle role in impacts. A parameter study of a simplified model of the head-neck complex with muscle elements is proposed here as a method for such analysis. This parameter study attempts to answer the following questions:

- How much do muscles affect the kinematics of the head-neck complex at different impact severity and for different reflex time?
- How dependent is the calculated influence of the muscles on the reflex time, and on an assumed initial tension in the muscles?
- Does the calculated influence of the muscles depend on the structure and parameters of the muscle models?
- How much does the calculated influence of the muscles depend on the static strength of the neck?

## 1.2 Methods

### 1.2.1 Models

#### Head-neck model

The aim of the current analysis is to perform a parameter study of the muscle effect. Such a study requires high number of computer runs to investigate the muscle effect for various values of different parameters. In this case computation time of each run is a critical factor. Therefore the authors developed only a simplified two-dimensional multibody model of the head-neck complex. The model is shown in Figure 1, and it is described in detail in Appendix 1. It consists of two rigid links: the head link and the neck link. The links are connected by two hinge joints: the neck link-torso joint, and the neck-head link joint. The head flexion/extension angle was defined as the angle in the plane of impact between the head link and the vertical axis fixed to the sled. The bases for modelling of the head-neck complex as a system of two rigid links were formulated by Wismans and Spenny (1984) and Wismans *et al.* (1986, 1987).

In the current study, all translational degrees of freedom of the head-neck complex were

left out, and only the “rotational kineto-static equilibrium”<sup>1</sup> of the head-neck complex was considered, see Eqs. (A1)–(A2) in the Appendix 1. The muscle effect was represented with torques generated by muscles about the neck-torso and head-neck joints. Thus, the torque about each joint consists of three components: the torque developed by muscles, the resistive torque related to passive stiffness, and the resistive torque related to passive damping. Torques developed by muscles were calculated with an assumption that the muscles’ moment arms do not change with movements of the head and neck. This assumption greatly simplifies the computational algorithms, and it makes possible to easily calculate a muscle elongation from a joint angular displacement. The latter is crucial to obtain input parameters for the muscle models, because the literature data on muscle characteristics are given in two forms: 1) as a muscle force—length relationship and 2) as a muscle torque—joint angle relationship (Winters and Stark, 1985; Winters and Stark, 1988; Winters et al. 1988). It is difficult to theoretically evaluate how much does the assumption about constant moment arms of muscles affect prediction of the muscle effect in frontal car collisions. However, in the authors’ opinion this assumption cannot significantly influence results of the current study. First of all, the moment arms of neck extensors do not change very much when the neck is flexing. Furthermore, the neck flexors do not play a significant role in resisting movements of the head and neck in frontal impacts. Therefore changes of the moment arms of flexors are not so important for the current study.

The complex system of the head-neck muscles was simplified and represented with three groups of flexors and three groups of extensors, see Figure 1 and Table 2. Maximum isometric torques/forces of muscles were calculated from the literature data. Total maximum

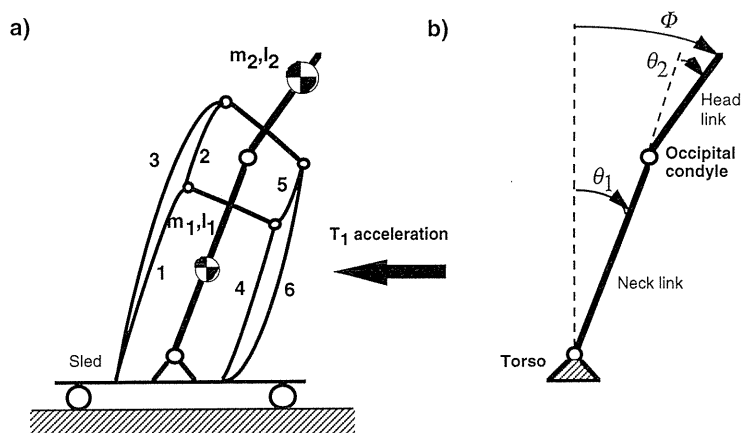


**Figure 1** The current model of the head-neck complex with muscle elements (curved lines). (a) Model with muscle elements (curved lines), see also Table 2. (b) Definition of flexion angles. Positive angle is flexion; negative one is extension.  $m_1$  and  $m_2$  are the lumped masses of the neck and head, respectively;  $I_1$  and  $I_2$  are the mass moments of inertia of the neck and head, respectively.  $T_1$  is the first thoracic vertebra.

<sup>1</sup>The authors realise that this term may not be precise enough. It is used to emphasise that only the rotational degrees of freedom were taken into account, and therefore only the joint torques were considered as generalised forces in equations of motion.

**Table 2** Muscle elements from the model shown in Figure 1. Each muscle element from the model represents lumped effect of the muscles specified in the column “Muscles”.

Muscle Element	Muscles
1	splenius cervicis, semispinalis cervicis, longissimus cervicis, levator scapulae (partly)
2	longissimus capitis, semispinalis capitis
3	trapezius (upper part)
4	scalenus
5	longus capitis, longissimus capitis
6	sternocleidomastoideus

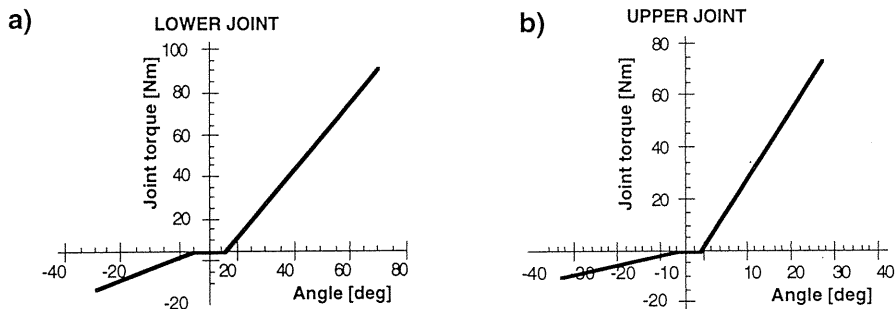


**Figure 2** Passive resistive joint torques. (a) Torque about lower joint, i.e. neck-torso joint. (b) Torque about upper joint, i.e. head-neck joint. Positive values of angle mean flexion; negative—extension.

isometric torques developed by the system of the neck muscles were estimated from the studies by Morehouse (1959), Mertz and Patrick, (1971) and Mayoux-Benhamou *et al.* (1989). Maximum static torque generated by flexors was assumed to be 50% lower than the maximum static torque generated by extensors (Morehouse 1959; Mertz and Patrick, 1971). Maximum force developed by a given muscle was calculated as a value proportional to the physiological cross-section area of the muscle. Physiological cross-section areas of the neck muscles were estimated from the data summarised by Yamaguchi *et al.* (1990). Passive stiffness of the neck-torso and the head-neck joints are based on the data by Bowman *et al.* (1984) and Wismans and Spenny (1984), see Figure 2. Damping coefficient of the head-neck joint is based on the results by Bowman *et al.* (1984).

Initial values of the neck-torso angle  $\theta_1$  and the head-neck angle  $\theta_2$  strongly influence dynamic response of the head-neck complex. In the current study, position of the head-neck complex prior to impact was treated as a constant. Initial values of  $\theta_1$  and  $\theta_2$  were selected to be  $18^\circ$  and  $-16^\circ$ , respectively. The basis for this selection is that these values were identified by Wismans *et al.* (1986) as average initial angles in the Naval Biodynamics Laboratory (NBDL) frontal impact tests.

The influence of muscle force on the maximum angle of the head flexion was analysed by investigation of changes of this angle caused by muscle action during 0.2 s of frontal impact. The following parameter was used as a measure of the relative influence of muscle force on the maximum angle of head flexion

$$Diff = \frac{\phi - \phi_{mus}}{\phi}, \quad (1)$$

where  $\phi$  is the maximum angle of the head flexion when the active function of the muscles is left out, and  $\phi_{mus}$  is the maximum angle of the head flexion when the active muscle force is generated.

### Reflex time and neural control

In the present study, the reflex time  $T_{reflex}$  was defined as the time between the  $T_1$  acceleration onset and the initiation of neuromuscular reaction. Thus, the impact pulse was interpreted as the stimulus. This definition yields the following form of the neurocontroller input signal  $u$ :

$$\begin{cases} u = 0 & t \leq T_{reflex} \\ u = 1 & t > T_{reflex} \end{cases} \quad (2)$$

The signal  $u$  is the input to equations which describe the dynamics of the neuromuscular excitation and the dynamics of the muscle active state (Winters and Stark, 1985, 1988):

$$T_{ne} \frac{dN_e}{dt} = u - N_e \quad \text{and} \quad (3)$$

$$T_a \frac{dN_a}{dt} = N_e - N_a, \quad (4)$$

where  $N_e$  is the neuromuscular excitation,  $N_a$  is the muscle active state,  $T_{ne}$  is the time constant of excitation, and  $T_a$  is the time constant of activation, see Figure 3 and Figure 4. According to Winters and Stark (1988) the activation and excitation time constants are in the range of  $0.005 \leq T_a \leq 0.020$  s and  $0.02 \leq T_{ne} \leq 0.05$  s, respectively. Based on these data the authors estimated  $T_a = 0.01$  s and  $T_{ne} = 0.035$  s for the neck muscles. In the current analysis, the original excitation-activation equations by Winters and Stark (1985, 1988) were modified with an assumption that the muscle active state is never lower than the minimum value  $A_{min}$  (Hatze, 1981; Pandey, 1990):

$$N_{am} = A_{min} + (1 - A_{min}) N_a \quad (5)$$

where  $N_{am}$  is the muscle active state after introducing the minimum value of the active state. Eq. (5) makes it possible to avoid singularities when solving the dynamic equations of muscle for low levels of the muscle active state. In the present study,  $A_{min}$  was assumed to be equal 0.005 which is a value proposed by Hatze (1981).



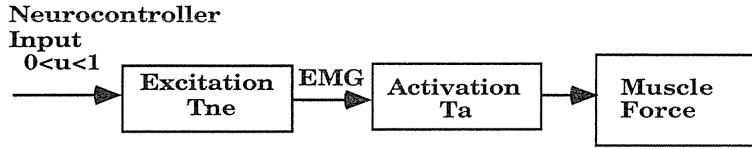


**Figure 3** Simplified scheme of the excitation-activation dynamics. EMG is an electromyographic signal. Based on Winters and Stark (1988).

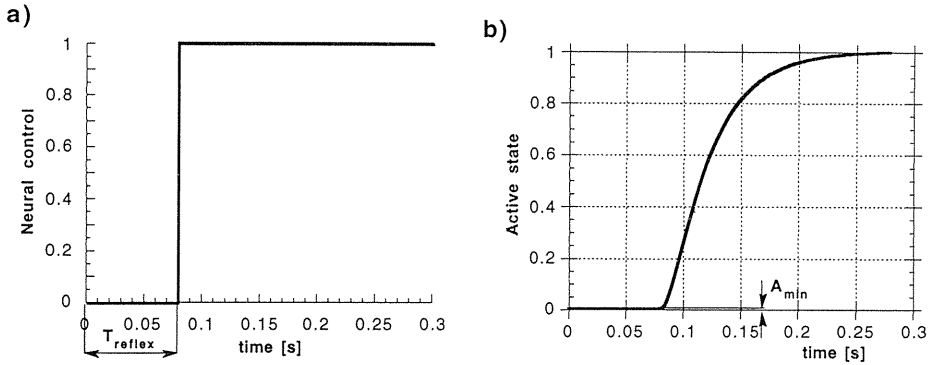


**Figure 4** (a) Neural control signal-time history. (b) Muscle active state-time history, i.e. solution of Eqs. (3)–(5).

### Muscle models

In the current study, the muscles were simulated by Hill-type models and a purely phenomenological model which treats muscle as a dynamic system of a given order, see Figure 5. Mathematical formulae to describe these models are presented in Appendix 2.

Structures A–D in Figure 5 are the Hill-type models. The structure A consists of contractile element and parallel element, and it describes muscle as a force generator within passive tissues. The structures B, C and D contain a series elastic element. In the structure C series elasticity of the muscle is separated from series elasticity of the tendon. From a mathematical point of view the main difference between the simple structure A and more advanced structures B, C, and D is that equations for dynamics of the structures with a series elastic element contain time derivative of muscle force. Whereas the muscle force of structure A is described with algebraic equation. The structure B is based on the studies by Winters and Stark (1985, 1988); the structure C is based on the study by Pandey *et al.* (1990, 1995). In the structure D muscle mass is taken into account. The series elastic element in this structure is interpreted as the tendon. Passive damping was implemented in the structure D to damp oscillations caused by the muscle mass. The muscle model with the muscle mass is described with second order ordinary differential equations. The structure D is based on the studies by Giat *et al.* (1994) and Shue (1995). Functions and parameters which determine the behaviour of Hill-type muscle models are based on the studies by Yamada (1970), Morgan (1977), Winters and Stark (1985), Winters and Stark (1988), Pandey *et al.* (1990), and Schneck (1992).

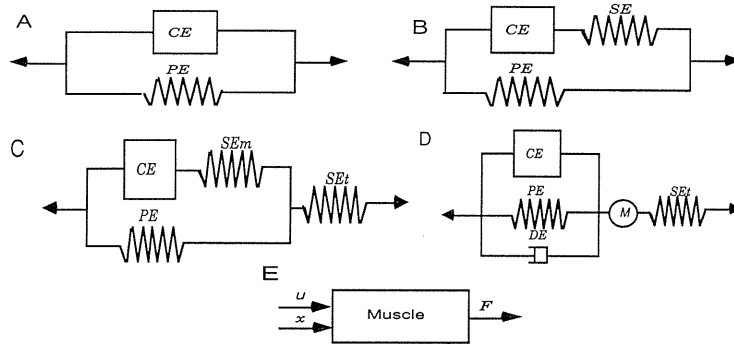


**Figure 5** Structures of muscle models used in the present study. Structures A, B, C, and D are Hill-type models. Structure E is a purely phenomenological “black box” model. *CE* is the contractile element, *SE* is the series elastic element, *PE* is the parallel elastic element, *SE<sub>m</sub>* is the series elastic element of the muscle, and *SE<sub>t</sub>* is the series elastic element of the tendon, *M* is the muscle mass, *u* is the neurocontroller input signal, *x* is the muscle elongation, and *F* is the active muscle force.

The model with structure E is based on purely phenomenological concepts which assume that a skeletal muscle is a dynamic system of second or greater order (Dabrowska and Kedzior, 1985; Kedzior and Lackowski, 1992). In the current study, a model of the second order was used. So far the model by Dabrowska and Kedzior (1985) has been applied only in the analysis of isometric muscle work when the passive function of muscle can be disregarded. The authors modified the model by Dabrowska and Kedzior (1985) by implementing a passive force component. The model E does not have any relation to a structure of a real muscle. It can be considered to be a “black box” with output interpreted as the muscle force.

### Impact pulses

The trunk was neglected in the current study. For this reason a horizontal acceleration of the first thoracic vertebra  $T_1$  was used as a loading pulse. The assumption that the  $T_1$  acceleration can be regarded as a load of the head-neck system has been widely used in the literature, e.g. Bowman *et al.*, (1984), Bosio and Bowman, (1986), and Wismans *et al.* (1986). The  $T_1$  acceleration-time histories used in the present study are based on published results of the frontal crash tests conducted on volunteers at the Naval Biodynamics Laboratory (NBDL). In the NBDL tests, subjects were seated in an upright position on an accelerator and exposed to short duration accelerations simulating frontal, oblique and lateral impacts. The resulting motions of the volunteers head and  $T_1$  were monitored by accelerometers and photographic targets. The NBDL experiments have been described and analysed in detail in many references, e.g. Wismans *et al.* (1986), Wismans *et al.* (1987), and Wismans *et al.* (1994).

### Programming and numerical methods

The programming was performed by means of *Mathematica* 2.2.2 software (Wolfram, 1993). The equations of motion of the head-neck model and dynamic equations of muscles were solved by using standard *NDSolve* procedure from the *Mathematica* software. *NDSolve*

uses Adams predictor-corrector method to solve non-stiff systems of ordinary differential equations, and Gear's method for stiff problems (Keiper, 1992). Computations were done on *SUN SPARC 20* workstation.

### 1.2.2 Parameter study of muscle influence

#### Influence of muscles at different impact severity and for different reflex time

Three impact pulses were used to analyse influences of muscles at different impact severity, see Table 3. Pulses *T12* and *T30* correspond to mean values of horizontal  $T_1$  acceleration-time histories in the NBDL frontal impact tests at peak sled acceleration 6 g and 15 g, respectively. Pulse *T70* is based on an upper bound of  $T_1$  horizontal acceleration in the NBDL frontal impact test at 15 g. This pulse was used to simulate a very severe impact.

**Table 3** Characteristics of impact pulses used in the current study.

Peak Sled Acceleration	Peak $T_1$ Acceleration	Symbol in text	Description	Reference
6 g	12 g	<i>T12</i>	Mean value from volunteer tests	Allen and Bowman (1986), Figure 4, page 349
15 g	30 g	<i>T30</i>	Mean value from the most severe volunteer tests	Wismans <i>et al.</i> (1994), Figure 5.13, page 93
15 g	70 g	<i>T70</i>	Envelope of volunteer tests	Wismans <i>et al.</i> (1987), Figure 5, page 5

Eight values of the  $T_{reflex}$  ranging from 0 to 0.2 s were used at each impact pulse, see Table 5.  $T_{reflex}=0$  corresponds to the situation when the nervous system reacts immediately after an impact onset. A reflex time lower than 0.06 s can be regarded to be a "fast" reaction of the nervous system. Since only initial 0.2 s of the impact were analysed for the impact pulses *T30* and *T70*,  $T_{reflex} \geq 0.2$  s corresponds to the situation when no muscle action is performed during the impact. At the impact pulse *T12* the head flexion angle reached maximum after 0.2 s. For this reason 0.3 s of an impact were analysed for this pulse. In this case  $T_{reflex} \geq 0.3$  s was used to model the situation when no muscle action is performed. The choice of values for the reflex time is based on results of the previous literature review (Wittek and Kajzer, 1995).

#### Influence of reflex time and initial muscle tension

The influence of the reflex time on the response of the model of the head-neck complex was analysed in more detail at the impact pulse *T30*. The time histories of the head flexion angle, the head angular acceleration, and the muscle force calculated for different reflex times were compared.

When the nervous system receives warning information before impact, the muscles can be activated at a high level in an initial impact phase to restrain injury-causing movement of the head-neck complex. Three sets of initial conditions were used to analyse the influence of initial tension. In the first set *TENS50*, the initial tension in the flexors was assumed to be 0.5 of the maximum isometric muscle force  $F_{max}$ , and the initial tension in the extensors was calculated to satisfy the equilibrium condition of the head-neck complex. In the second set *TENS80E*, the initial tension in the muscle (2), see Figure 1, was assumed to be  $0.8F_{max}$ ,

while the initial tension in other muscles was  $A_{min}F_{max}$ . In the third set *TENS80*, the initial tension was assumed to be  $0.8F_{max}$  in all the muscles. In the sets *TENS80E* and *TENS80*, the equilibrium conditions were not satisfied, and the muscle tension forced the head-neck complex to move backward. The authors have found no relevant data in the literature to analyse the influence of initial muscle tension. The assumptions just presented are based on an arbitrarily choice by the authors.

### Influence of structure and parameters of muscle models

The influence of the structure of the muscle model was analysed at the impact pulse *T30*. The reflex time was selected to be zero. Time histories of the head flexion angle and the muscle force were calculated for five structures of the muscle models, and then they were compared. The structures of the muscle models are shown in Figure 5.

The influence of the parameters of the muscle model was investigated for the Hill-type model with structure B. This structure was selected to be a reference structure of the muscle model for two reasons. First, this structure has been widely used in the literature and many parameters for this structure have been determined (Winters and Stark 1985, 1988). Second, it requires less computation time than the more complex structure C. The influence of the following parameters was analysed: maximum shortening velocity of the contractile element  $v_{max}$ , shape parameter of the force—strain characteristics of the series elastic element  $C_{SE}$ ,

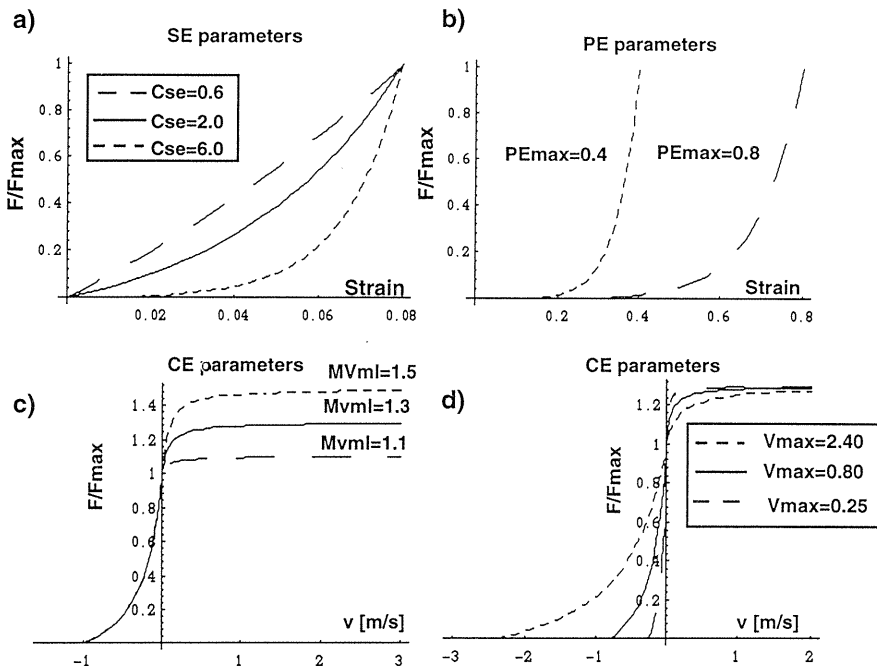


**Figure 6** Characteristics of Hill-type model with structure B for different parameters. (a) Series element force for different values of  $C_{SE}$ , (b) Parallel element force for different values of  $PE_{max}$ , (c) Force—velocity relation for different values of  $MV_{ml}$ , and (d) Force—muscle velocity relation for different values of  $v_{max}$ .  $F$  is the muscle force,  $v$  is the muscle velocity and  $F_{max}$  is the maximum isometric force.

strain of the parallel elastic element at the maximum isometric force  $PE_{max}$ , and parameter  $MV_{ml}$  which describes how many times the force during active lengthening is asymptotically greater than the isometric force.

In the current study the strain of the parallel elastic element is calculated in the reference to the optimum muscle length. The optimum length is the length at which generation of the active muscle force is the most efficient. Some basic effects of the muscle model parameters on the behaviour of the muscle model are shown in Figure 6. The reference values of the parameters were based on the average of the literature data (Winters and Stark, 1985; Winters and Stark, 1988; Lehman, 1990). The lower and upper bounds were slightly out of the range of the literature data, see Table 4.

**Table 4** Test matrix for analysis of the influence of the muscle model parameters.

Parameter	Lower bound	Reference value	Upper bound
$C_{SE}$ (Figure 6a)	$0.3 \cdot (\text{reference value})$	2.0	$3 \cdot (\text{reference value})$
$PE_{max}$ (Figure 6b)	$0.3 \cdot (\text{reference value})$	0.8 of the optimum muscle length	reference value
$MV_{ml}$ (Figure 6c)	1.0	1.3	1.8
$v_{max}$ (Figure 6d)	$0.3 \cdot (\text{reference value})$	0.8 m/s	$3 \cdot (\text{reference value})$

### Influence of the static neck strength

In the current study, the static neck strength was defined as the maximum static torques generated by the muscles about the neck-torso joint and about the occipital condyles. Based on the literature review, the following data on the maximum static torques were selected for investigation of the influence of the static neck strength:

- 1) 30 Nm for neck extensors and 15 Nm for head extensors;
- 2) 65 Nm for neck extensors and 30 Nm for head extensors;
- 3) 100 Nm for neck extensors and 50 Nm for head extensors.

Maximum torque of neck extensors equalled 30 Nm can be regarded as a low value which corresponds to elderly persons. Whereas a value of 100 Nm corresponds to young, well-trained subjects. Data from point (2) are an average of the literature data, and they were selected to be reference values.

### Test Matrix

Tests for the analysis of the influence of different factors on the muscle effect result in 76 computer runs. They are summarised in Table 5.

### Head-neck model validation

The head-neck model was validated by comparison of the calculated head flexion angle and the head angular acceleration-time histories with the envelopes of the NBDL experimental results presented by Wismans *et al.* (1987). Direct validation of the calculation of muscle force was not possible because of lack of the experimental data on muscle tension.

**Table 5** Test matrix for analysis of influence of different factors on the calculated effect of muscles on the response of the head-neck model.

Analysed factor	Values for analysed parameter	Number of runs	Summary
Impact severity for different reflex time	12 g, 30 g, 70 g; See pulses <i>T12</i> , <i>T30</i> , <i>T70</i> in Table 3	24	Horizontal acceleration of $T_1$ from NBDL volunteer tests at 6 g and 15 g sled acceleration. Analysis was done for structure B of muscle model.
Reflex time	0.00 s, 0.02 s, 0.04 s, 0.06 s, 0.08 s, 0.10 s, 0.12 s, 0.20 s	8	Analysis was done for the muscle model, with structure B. The head-neck complex was loaded by impact pulse <i>T30</i> .
Initial tension in muscles	$0.5 F_{max}$ , $0.8 F_{max}$	2	Influence of initial tension was investigated for the muscle model with structure B. The head-neck complex was loaded by impact pulse <i>T30</i> .
Structure of muscle model	see Figure 5	32	Analysis was done at loading pulse <i>T30</i> . Five structures of the muscle model were investigated.
Parameters of muscle model: $v_{max}$ , $C_{SE}$ , $PE_{max}$ , $MV_{ml}$	see Table 4	8	Parameters of muscle model were investigated for the muscle model with structure B. The head-neck complex was loaded by impact pulse <i>T30</i> .
Static strength of the neck [Nm]	Neck-torso joint 30, 60, 100 Head-neck joint 15, 30, 50	2	Influence of static strength was investigated for the muscle model with structure B. The head-neck complex was loaded by impact pulse <i>T30</i> .

### 1.3 Results

#### 1.3.1 Influence of muscles at different impact severity and for different reflex time

Influence of muscles on response of the head-neck model greatly decreased when the impact severity increased. The maximum angle of the head flexion was reduced by up to 65% at the impact pulse *T12*, and only by about 20% at the impact pulse *T70*, see Figure 7

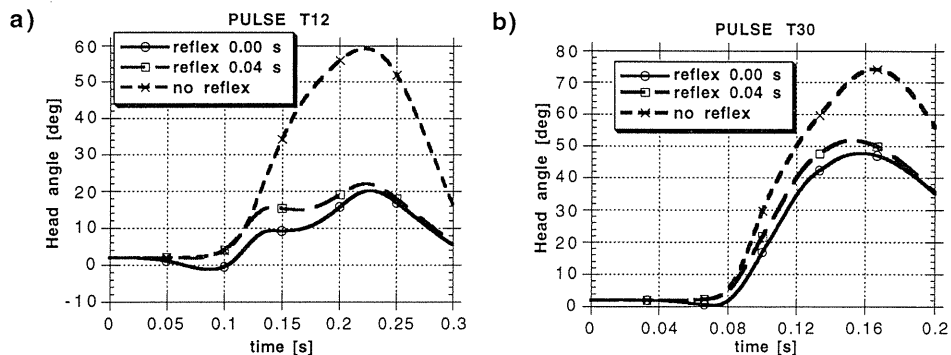


**Figure 7** Head flexion angle-time histories at different impact severity and for different reflex time. (a) Load pulse *T12*. (b) Load pulse *T30*.

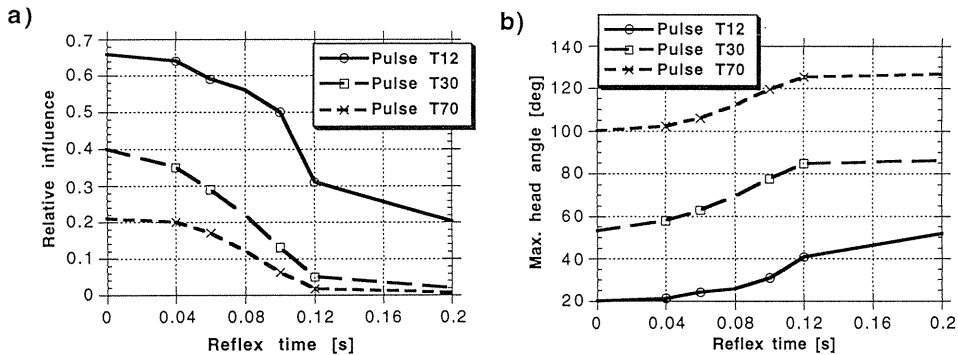


**Figure 8** Influence of muscles on the head flexion angle as a function of the reflex time at different impact severity. (a) Relative changes of the maximum angle of head flexion (parameter *Diff*). (b) The maximum angle of head flexion.

and 8. At impact pulses *T30* and *T70* relative influence of muscles dropped to a value lower than 15% when  $T_{reflex}$  was greater than 0.12 s, see Figure 8.

#### Influence of reflex time and initial muscle tension

When the reflex time was lower than 0.04 s, muscles decreased the maximum angle of head flexion by about 40% at the impact pulse *T30*, see Figure 8a and Figure 9a. However, the maximum angular acceleration of the head was reduced by muscle tension only by about 10%, see Figure 9b. Thus, the peak value of the head angular acceleration was probably more affected by characteristics of an impact pulse itself and passive properties of joints than by forces generated by the muscles.

For the reflex time greater than 0.10 s the maximum force in extensors was calculated to be lower than  $0.8F_{max}$ , and relative influence of muscles was lower than 20%. Furthermore, the force in extensors quickly dropped after the first peak, see Figure 10. In consequence, muscles could not significantly affect kinematics of the head-neck complex for high values of the reflex time.

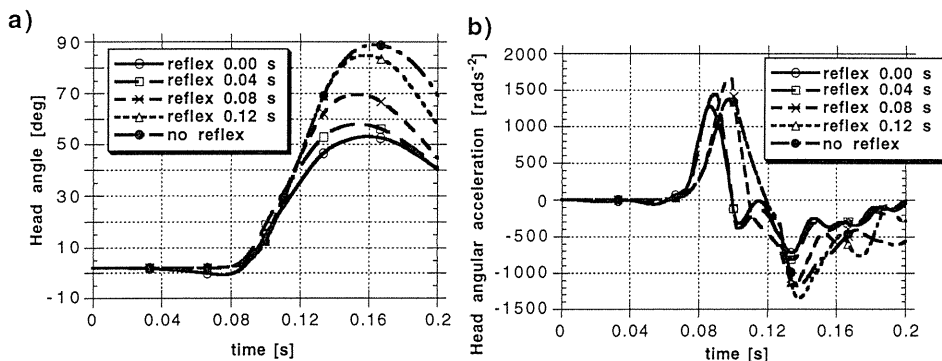


**Figure 9** Results for impact pulse *T30* for different values of the reflex time. (a) Angle of head flexion (b) Angular acceleration of the head.

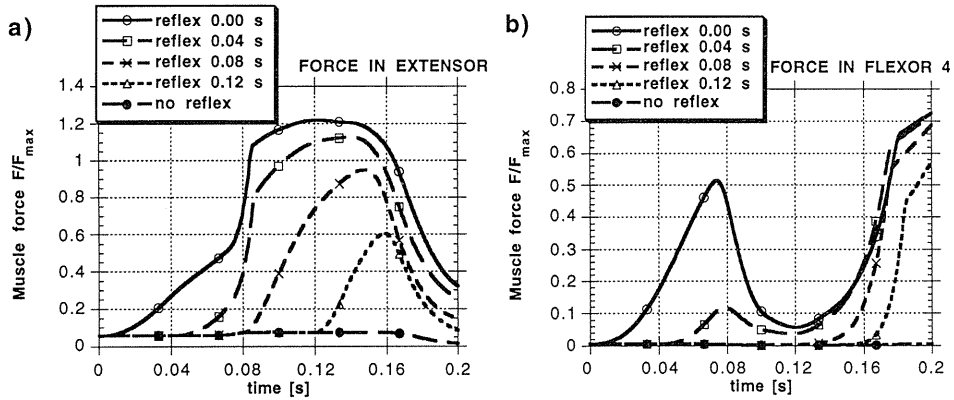


**Figure 10** Muscle-force time histories for different reflex time. (a) Muscle 1 (extensor). (b) Muscle 4 (flexor). Force is normalised to  $F_{max}$ .

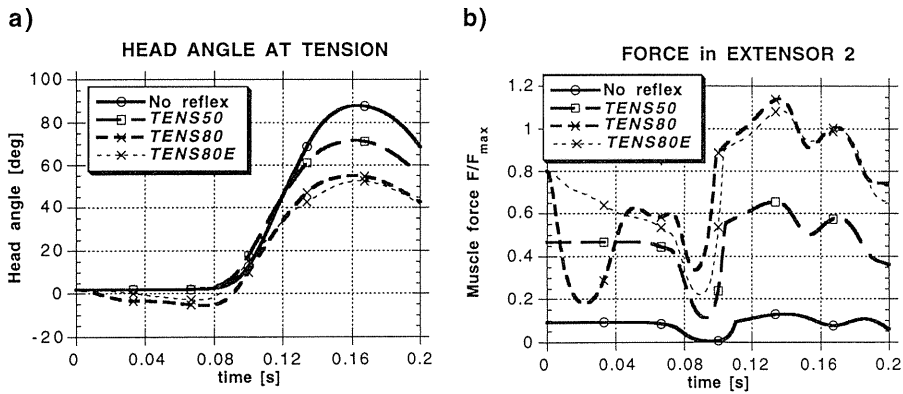


**Figure 11** Influence of initial muscle tension on the head-neck model response (a) Angle of head flexion and (b) Force in muscle 2.

High initial tension in muscles did not reduce the maximum angle of the head flexion in comparison to the initial conditions with the initial tension calculated as  $A_{min}F_{max}$  and  $T_{reflex}=0$ , see Figure 11. High initial tension in extensors led to large extension of the head in relation to the neck. In consequence, the head angle-time histories exhibited negative values in the initial phase of the impact, see Figure 11a. The results just described are compatible with the findings by Bosio and Bowman (1986) who suggested that large head extension in the NBDL experiments can be related to muscle action.

### Influence of structure and parameters of muscle models

Significant differences were found in responses of the head-neck model with muscles modelled by Hill-type models and the muscles modelled by a “black box” model of the second order. The latter exhibits more “inertial properties” and requires longer time to generate



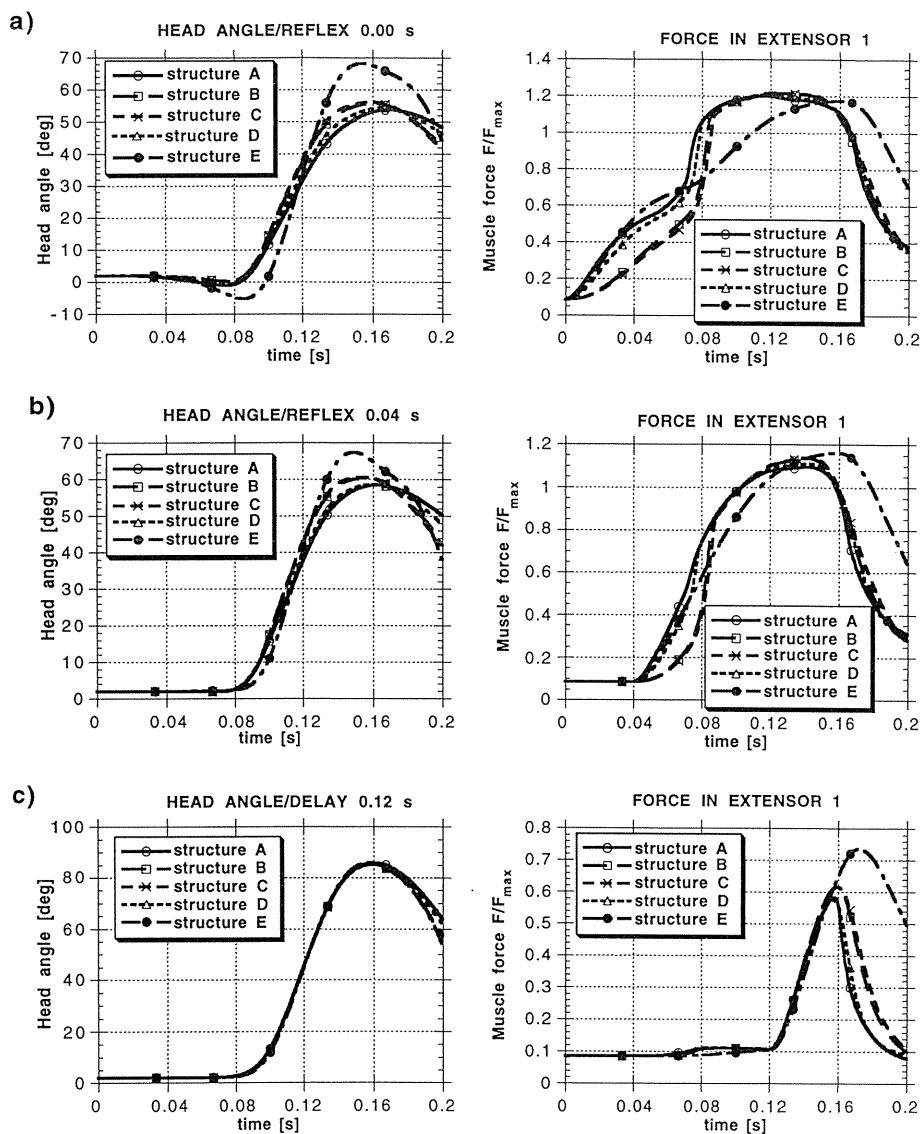


**Figure 12** Influence of structure of the muscle model on head flexion angle-time histories (left side) and muscle force-time histories (right side) for different reflex times. Structures of the muscle model are shown in Figure 5. (a) Reflex time 0 s. (b) Reflex time 0.04 s. (c) Reflex time 0.12 s.

a high muscle force, see Figure 12. In consequence, the maximum angle of head flexion was greater for the “black box” muscle model than for the Hill-type models.

Responses of Hill-type models with series elastic element and without series elastic element were slightly different. In the models with the series elastic element the muscle force went up more slowly in the beginning of an impact, and then increased more steeply than in

the model without series elastic element, see Figure 12. This phenomenon is related to the exponential relation between force and elongation of the series elastic element. When the elongation is less than about 0.01 of the muscle length at rest, the force in the series elastic element is very close to zero. When the elongation continues, the force quickly increases, and reaches a value of the maximum isometric force at elongation corresponding to about 0.03–0.05 of the muscle length at rest.

The results from the model with the muscle mass, structure D, did not significantly differ from the other models, except muscle force-time histories for long reflex time. The muscle model with mass exhibited oscillations when the reflex time was greater than 0.1 s, see Figure 13. For the reflex time shorter than 0.06–0.08 s, the muscle stiffness was relatively high in the initial phase of the impact, which prevented the model from oscillations with a large amplitude, see Figure 14. An effect of a muscle mass depends on passive damping of the muscle, and increased when the mass was heavy. Comparison of the results for the total mass of the neck muscles equalled 0.5 kg and 5 kg is presented in Figure 13. The mass of 0.5 kg is an average value based on the literature data (Pitman and Peterson, 1989), and it corresponds to the mass of about 0.1 kg for each muscle element. With this value oscillations of

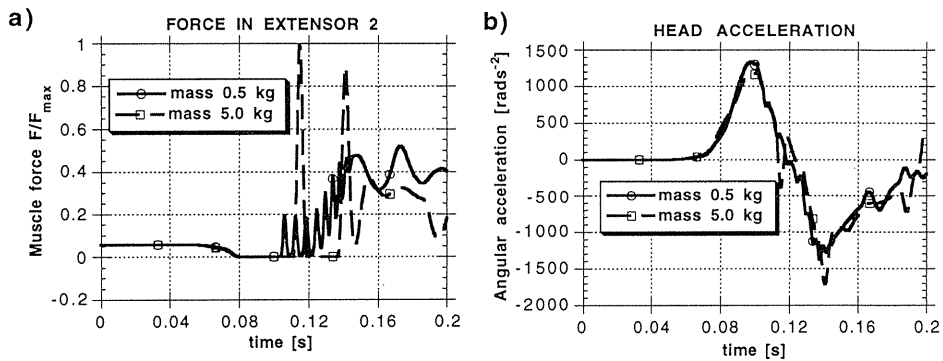


**Figure 13** Influence of the muscle mass on the muscle force-time histories and the model kinematics for the reflex time 0.12 s. (a) Muscle force-time histories of extensor 2. (b) Head angular acceleration.

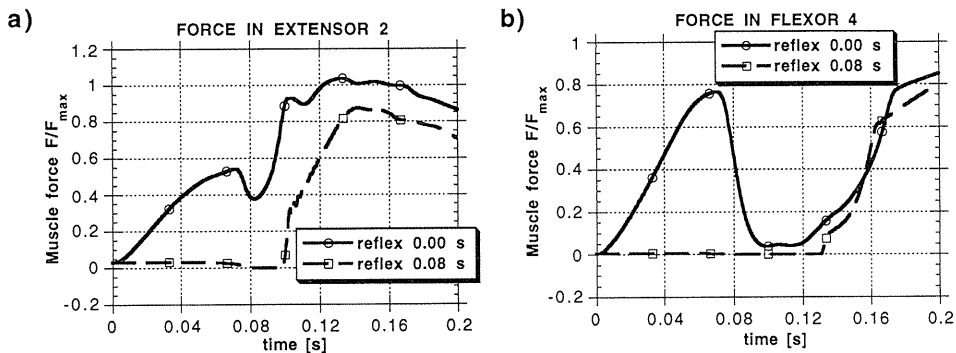


**Figure 14** Muscle force-time histories of the model with total mass of the neck muscles 0.5 kg for different reflex times. (a) Results for extensor 2. (b) Results for flexor 4.

the muscle model were not strong enough to affect kinematics of the entire head-neck complex. The value of 5 kg was selected arbitrarily to represent very heavy muscle mass. With this value oscillations of the muscle model strongly affected the angular acceleration-time histories. The authors have found no experimental data to evaluate to what extent the oscillations reported here correlate with the behaviour of real muscle. At this stage of the study of muscle effect in impacts it can be concluded only that the results of mathematical modelling can be strongly affected by a magnitude of the muscle mass.

Analysis of influence of muscle model parameters indicate that for high values of  $C_{SE}$  muscle-force time curves were slightly shifted towards the right on the time-axis, see Figure 15b. The reason for this shift is that the stiffness of series elastic element greatly decreases for low values of  $C_{SE}$ , see Figure 6a. Since a muscle elongation is the sum of the elongation of the series element and the contractile element, the elongation of the contractile element decreases when the stiffness of the series elastic element is low, see Eqs. A2.12–A2.16 in the Appendix 2. In general, the head angle-time histories were not sensitive to  $C_{SE}$ . Variation of  $C_{SE}$  by 10 times resulted only in a 5% difference in the maximum angle of head flexion, see Figure 15.

The current results show that the maximum shortening velocity  $v_{max}$  can relatively

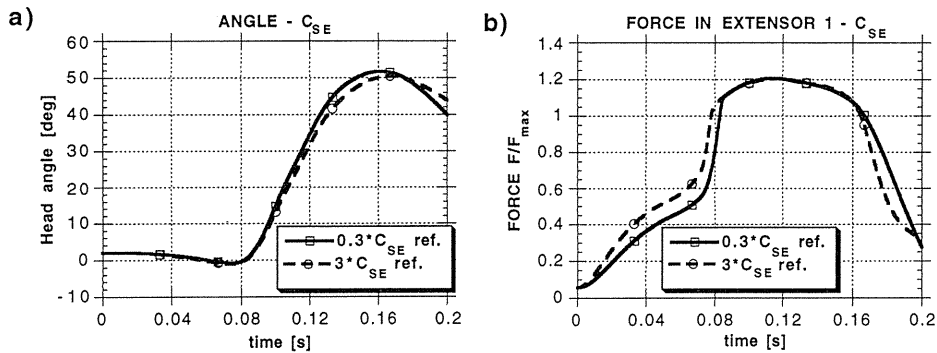


**Figure 15** Influence of  $C_{SE}$ . (a) Head flexion angle-time histories and (b) Muscle force-time histories for different values of  $C_{SE}$ .

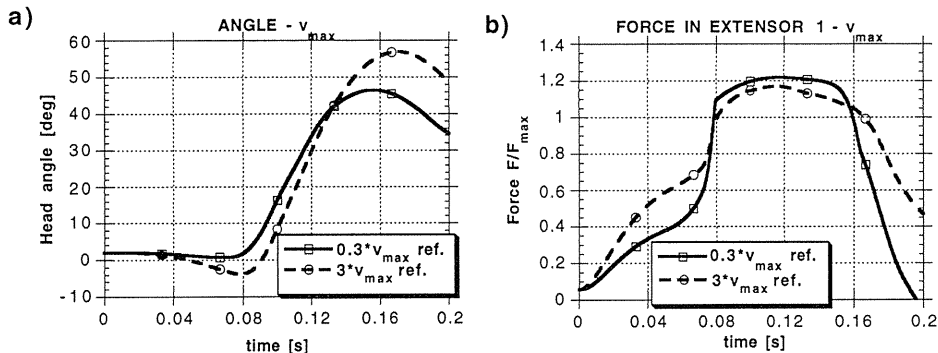


**Figure 16** Influence of  $v_{max}$ . (a) Head flexion angle-time histories and (b) Muscle force-time histories for different values of  $v_{max}$ .

strongly affect muscle force-time histories. Influence of  $v_{max}$  was the most evident in the initial phase of impact, see Figure 16. The explanation is that  $v_{max}$  significantly affects the force-velocity characteristics when the muscle performs concentric work. Such concentric work can be performed by extensors during first 0.01 s of impact when the impact pulse  $T30$  does not reach high values. Since the calculated peak value of muscle force only slightly changes with  $v_{max}$ , variation of  $v_{max}$  by 10 times exerted only a 20% influence on the maximum angle of the head flexion.

The peak value of force generated by the muscle during its eccentric work is proportional to the parameter  $MV_{ml}$ , see Figure 6c. In the current study frontal impacts only were analysed. In frontal impacts, the behaviour of the neck extensors is dominated by the eccentric work. In consequence, the peak value of muscle force increased, and the maximum angle of the head flexion decreased when  $MV_{ml}$  increased, see Figure 17.

For low values of  $PE_{max}$  the calculated passive force reaches significant values at low muscle elongation, see Figure 6b. In the current study, the peak value of the muscle elongation was about 0.5 of the muscle length at rest. At this level of elongation muscle force reached unrealistically high values when the assumed  $PE_{max}$  was less than 0.3–0.35 of the optimum muscle length, see Figure 18.

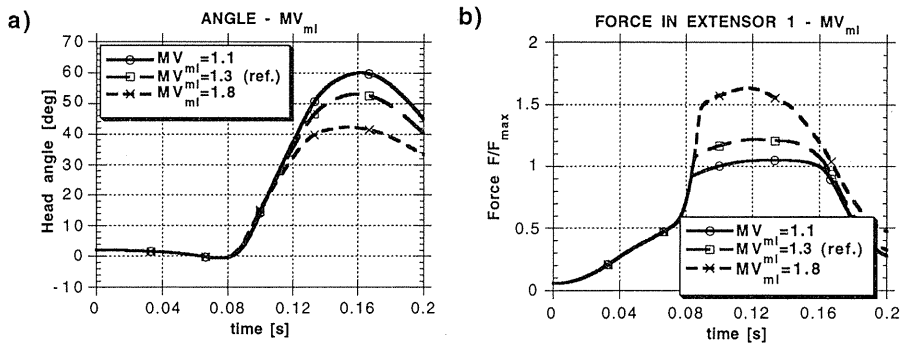


**Figure 17** Influence of  $MV_{ml}$ . (a) Head flexion angle-time histories and (b) Muscle force-time histories for different values of  $MV_{ml}$ .

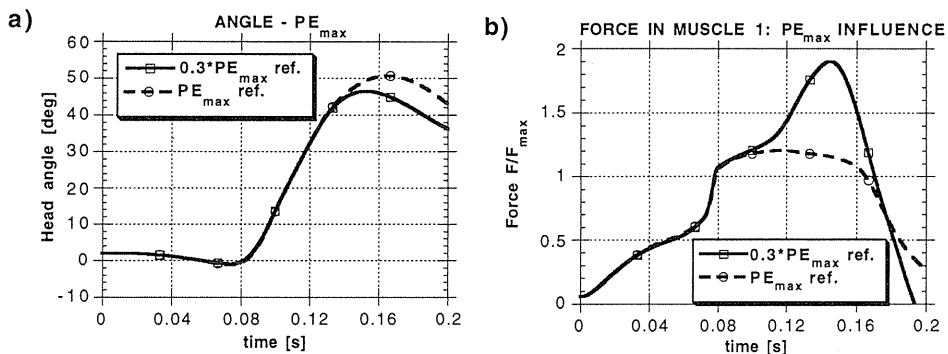


**Figure 18** Influence of  $PE_{max}$ . (a) Head flexion angle-time histories and (b) Muscle force-time histories for different values of  $PE_{max}$ .

### Influence of static neck strength

Effect of muscle force on the maximum angle of head flexion was almost linearly dependent on the static neck strength, see Figure 19. Maximum angles of the head flexion were 36°, 53°, and 73° for the maximum static torques of the neck extensors 100 Nm, 65 Nm, and 30 Nm, respectively.

### Results of validation

The envelope of the head flexion angle-time histories calculated in the present study well correlates with the NBDL experimental results by Wismans *et al.* (1987), see Figure 20. The current model of the head-neck complex well predicts the peak angle of the head flexion. On the other hand, the current results differ from the NBDL results in two important points:

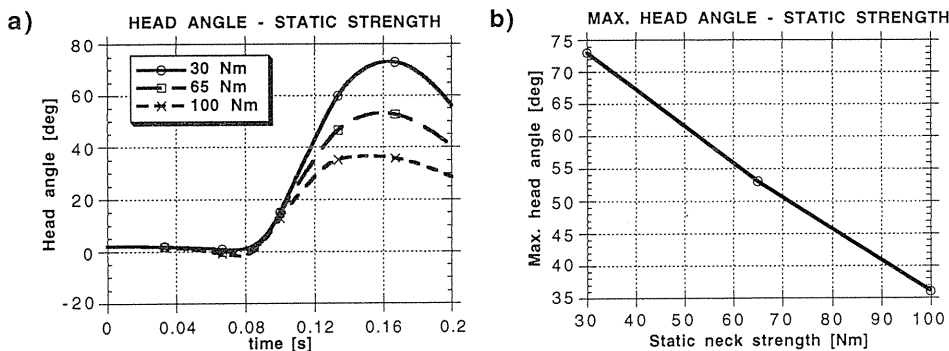


**Figure 19** Influence of the static neck strength at impact pulse *T30*. In this figure, the term static neck strength is referred to the maximum static torque of extensors. (a) Head flexion angle-time histories for different values of the static neck strength. (b) Maximum angle of head flexion as a function of the static neck strength.

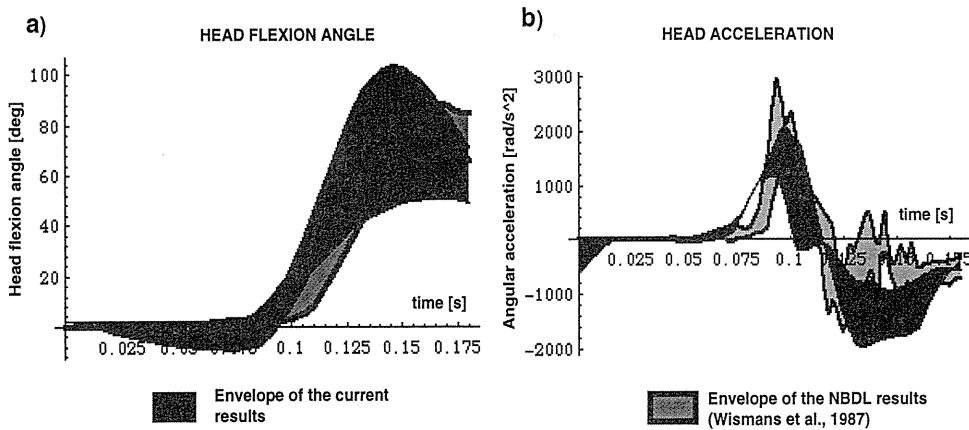


**Figure 20** Envelopes of the current results and the experimental results by Wismans *et al.* (1987). (a) Angle of head flexion. (b) Angular acceleration of the head.

1) Lower bound of the present time histories of the head flexion angle exhibits negative values; and 2) The peak angular acceleration is slightly lower in the present study than in the NBDL experiments, see Figure 20. The differences just described are related to five important simplifications of the current model of the head-neck complex.

First, the rotation of the first thoracic vertebra during impact was neglected. Second, complex structure of the neck was modelled as a single rigid link. Third, the head-neck model has only rotational degrees of freedom. The translational displacements of the first thoracic vertebra were disregarded. Fourth, characteristics of loading pulses, mass properties of the head-neck model, characteristics of the passive joint torques, and initial position of the head-neck complex were estimated here as the average values of the literature data. Such an estimation is deficient to predict the whole envelope of biodynamic responses of the human subjects. Fifth, possible differences in the reflex times between flexors and extensors were left out. It was assumed that all the muscles start to react at the same time, and that they are controlled by the same motoneuron.

#### 1.4 Discussion

The results of the present study indicate that muscles can significantly affect kinematics of the head-neck complex in 15 g frontal impact when the following conditions are satisfied simultaneously:

- Peak of  $T_1$  horizontal acceleration is less than 70 g;
- Reflex time is lower than 60 (80) ms.

When these conditions were satisfied, the maximum angle of the head flexion was decreased by muscle tension by up to 40%. When the peak of  $T_1$  acceleration was about 70 g, muscles were not able to significantly influence kinematics of the head-neck complex, even for very low values of the reflex time. Peak linear acceleration of  $T_1$  equalled 70 g corresponds to the upper bound of the NBDL experiments in 15 g frontal impact. It is reasonable to expect that the  $T_1$  acceleration can reach much higher values when the peak of the sled acceleration is greater than 15 g. Thus, it can be concluded that the muscle effect is negligible in frontal impacts which are more severe than 15 g.

The tendency of the current results agrees well with experimental and simulation results which have been reported in the literature. Kinematics of the present model of the head-neck complex exhibits good correlation with the NBDL data by Wismans *et al.* (1987), see Figure 20. The level of muscle influence calculated here is close to the experimental results by Mertz and Patrick (1967, 1971) presented in Table 1, and to the results of mathematical modelling by Pontius and Liu (1976) and Happee and Thunnissen (1994a). On the other hand, the current study shows that muscles do not significantly decrease maximum angular acceleration of the head, which is contrary to the experimental data by Verriest *et al.* (1975), who found that muscle force can reduce the peak value of head angular acceleration by about 40% in 20 g frontal impact. The authors propose the following explanations: 1) There are differences in characteristics of impact pulses between the experiments by Verriest *et al.* (1975) and the present analysis; and 2) The study by Verriest *et al.* (1975) was done on baboons. Hence their results cannot be directly extrapolated to humans.

The results of the current study indicate that kinematics of the head-neck complex strongly depends on the assumed initial tension in muscles. Therefore pre-impact activity of the neck muscles should be taken into account in the analysis of the muscle effect on the kinematics of the head-neck complex in a car crash.

The muscle force-time histories calculated in the current study do not strongly depend on structure of the muscle model. Significant differences were found only between Hill-type

models and "black box" model of the second order. The "black-box" model needs longer time to generate significant force, which affects the kinematics of the head-neck model. There were also some differences in response of the Hill-type models with series elastic element and without series elastic element. However, differences between various kinds of the Hill-type models were not strong enough to significantly affect structural response of the model of the head-neck complex. The influence of structure of the muscle model reported here is much lower than the influence calculated by Audu and Davy (1985). Their study has shown that results for the muscle model with series elastic element differ strongly from those for the model without series elastic element. One explanation could be that Audu and Davy (1985) analysed kinematics of kicking, and their findings cannot be extrapolated to transient loads.

The current results suggest that the structural response of the head-neck model does not strongly depend on most parameters of the muscle models. The shape parameter of force-elongation characteristics of the series elastic element  $C_{SE}$  exerted only a minor influence on the muscle force-time histories. This finding is consistent with the results of Winters and Stark (1985) who found that results of modelling of fast ballistic movements of the human extremities exhibit a very low sensitivity to  $C_{SE}$ . The maximum shortening velocity of the contractile element  $v_{max}$  does not significantly influence head angle-time histories. However, as this parameter directly affects muscle force-time histories, it is reasonable to expect that its influence would increase at low impact severity. Both the kinematics of the head-neck complex and the muscle force-time histories were relatively strongly affected by the parameter  $MV_{ml}$  which represents force during active lengthening of the muscle in relation to the isometric force. Thus, the present study shows that the force-velocity characteristics can be relevant in the analysis of the muscle response to transient loads. Similar findings have been reported by Winters and Stark (1985) and Winters *et al.* (1988) in the analysis of response of the elbow system to transient loads.

The static neck strength was identified as a biomechanical parameter which has the strongest effect on the calculated influence of muscles on the head-neck complex kinematics. The calculated maximum angle of head flexion was almost linearly dependent on the static neck strength.

There are some important limitations of the present results. First, the current model of the head-neck complex underestimates angular acceleration of the head. Second, calculation of muscle force was not directly validated because of lack of the relevant experimental data. Despite the limitations just described the results of the current study are compatible with the experimental literature.

In summary, the present study indicates that muscle effect may be negligible at impact pulses which are more severe than 15 g and for reflex times greater than 100 (120) ms. The calculated influence of muscles was not very sensitive to the structure and the parameters of the muscle model. Significant differences were found only between Hill-type models and the "black box" model of the second order. Only the static neck strength and the parameter which represents force during active lengthening in relation to the isometric force were identified as the parameters which can have a strong influence on the calculated effect of muscles. Those two parameters determine directly a maximum force of the muscle model. Therefore their strong effect on simulation results can be predicted even intuitively.

Thus, the authors suggest that the parameters and the structure/complexity of the muscle models are not the key points in the analysis of the muscle effect on the kinematics of the head-neck complex in a car crash. However, it is necessary to realise that the validity of the current conclusions is limited to the models which treat the muscle as a one-dimensional actuator with point mass. Such models have important disadvantages. For instance, they are deficient to realistically analyse the effect of the muscle mass. They also lack accuracy in

description of a contact between muscles and the skeleton, which can lead to errors in calculation of moment arms of muscle forces about the joints. Therefore in-depth investigation of the muscle influence on the head-neck complex kinematics necessitates to develop a more advanced structural model of the neck muscles and the model of the head-neck complex with accurate geometry. In the authors' opinion, the finite element analysis is a suitable tool for such a development.

Since the system of the neck muscles consists of several layers of muscles which are located at different distances from the skin, information about activity of the muscles which are distant from the skin can be needed in a validation of a refined finite element model of the head-neck complex. So far the surface electromyography technique has been used in the analysis of the neck muscles activity in a car crash, *e.g.* the study by Szabo and Welcher (1996). This technique applies electrodes which are placed on the skin. It is deficient to assess the activity of muscles that are distant from the skin. Therefore the authors suggest that the fine wire electromyography may be necessary in order to obtain in more detail data on the activity of the muscles in a car crash.

The most important technical limitation of the current study is that the *Mathematica* software was used as a programming and simulation tool. The *Mathematica* software makes it possible to efficiently program and perform calculation of different mathematical problems. It has not been optimised to solve specific problems. In consequence, for the calculations performed in the current study the computation times were relatively long, and the internal memory requirements were high. For these reasons the *Mathematica* is deficient in development of an advanced model of the head-neck complex with a refined structure and geometry. Such a development necessitates to use specialised simulation tools, such as transient dynamics explicit finite element codes, *e.g.* PAM-CRASH (ESI, 1996) or DYNA3D (Hallquist, 1992).

Thus, the authors propose that further in-depth analysis of the muscle effect in impacts should be focused on the following topics: investigation of possible influence of the muscle mass, development of refined structural model of the head-neck complex and the neck muscles, and experimental study on the activity of the neck muscles in a car crash. The authors propose that the modelling part of such an analysis can be performed with commercial finite element codes for simulation of transient dynamics problems, and the experimental part can be performed with the fine wire electromyography technique. Development of Hill-type finite element model of a skeletal muscle is discussed in Chapter 2.

## **Chapter 2. Development of a Hill-type Finite Element Muscle Model for Investigation of the Human Body Response Under Transient Load**

### **2.1 Introduction**

Commercial finite element (FE) codes facilitate development of models of the human body and the human body substitutes with accurate geometry (Fredriksson, 1996). On the other hand, such codes lack material models which can capture whole spectra of complex responses of skeletal muscles and other living tissues subjected to transient loads. For this reason, several attempts have been made to develop highly specialised codes which enables modeling of active function of skeletal muscles under transient loads, *e.g.* Pontius and Liu (1976), Williams and Belytschko (1983). Since such codes are developed primarily for scientific purposes, they often lack compatibility with commercial software currently used by car manufacturers. Therefore the possibility of their industrial application is limited. An



alternative solution is to implement material models of living tissues in commercial codes used in a field of car crash safety. Such a solution makes it possible to use the same simulation tools for modelling of both the car structure and the human body.

Dynamic analysis of mechanical systems can be performed with various kinds of FE software which use different methods to solve equations of motion: explicit, implicit and modal methods. In the field of car crash safety, explicit FE codes, such as LS-DYNA3D (Hallquist et al., 1991), PAM-CRASH (ESI, 1996) and RADIOSS (Mecalog, 1994), are the most common. In the current study, the PAM-CRASH code was selected as a software tool for the implementation of a muscle model.

A skeletal muscle can be mathematically analysed with various kinds of models which strongly differ in their complexity, *e.g.* phenomenological models that treat muscle as a dynamic system of a given order (Kedzior and Lackowski, 1990), Huxley cross-bridge model which is based on biophysiology of muscle contraction (Huxley, 1957, Huxley, 1969, Huxley and Simmons, 1971), and Hill-type muscle models (Hill, 1938, Winters, 1990). In the current study, the Hill-type model was selected for the implementation in PAM-CRASH. This selection is based on the previous literature review which has shown that the Hill-type models are much less complex than the Huxley-type models, and simultaneously they are capable of capturing the essential features of activated muscle behaviour (Wittek and Kajzer, 1995).

The goal of the current investigation is to implement a Hill-type muscle model in explicit transient dynamics FE code PAM-CRASH. Furthermore, we analysed responses of that FE muscle model to transient loads and we performed some basic tests to investigate the model reliability.

## 2.2 Methods

### 2.2.1 Mathematical formulae for Hill-type finite element muscle model

The muscle model by Hill (1938) is only a conceptual idea, and its elements cannot be assigned to particular anatomic structures with any certainty. This results in various structures of the Hill-type models and differences when identifying their parameters. Several examples of different structures of Hill-type models were analysed in Chapter 1 and in the previous literature review (Wittek, 1995). Based on this analysis, the Hill-type model with the structure of Figure 21 was selected for the implementation in PAM-CRASH code. This model is

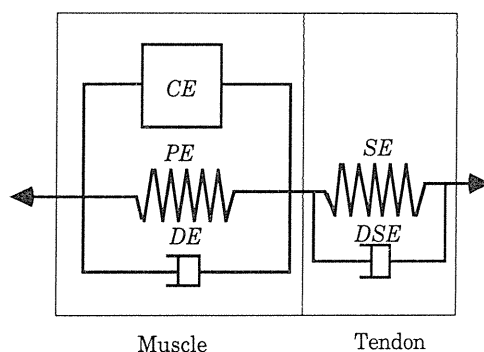


**Figure 21** Hill-type muscle model used in the current implementation of the FE muscle model in PAM-CRASH. *DSE* is damping of the series elastic element.

directly based on the model D of Figure 5 of Chapter 1. The model of Figure 21 consists of the following elements: contractile element *CE* which simulates active muscle force, parallel element *PE* which accounts for the muscle passive function, parallel damper *DE* which simulates viscoelastic properties of the muscle, series elastic element *SE* and damping of the series elastic element *DSE*. In this model, the series elastic element is interpreted as a tendon. The model of Figure 21 was selected for implementation in FE code for two important reasons:

- 1) Results presented in Chapter I of the current report indicated that such a model well simulates the crucial features of skeletal muscle behaviour, such as an effect of series elasticity, force—velocity and force—length characteristics. Simultaneously, computational cost of this model is relatively low.
- 2) The model shown in Figure 21 can be easily separated in two distinct types of finite elements: muscle with contractile element *CE* and tendon *SE*. This, in turn, simplifies numerical implementation of this model in FE codes.

The only one structural difference between the model D of Figure 5 and the model of Figure 21 is that in the latter *SE* damping is taken into account. The reason for taking into account the *SE* damping in the current formulation of a FE muscle model is that an analysis of the human body response to transient loads requires to model muscle behaviour at a high rate of deformation. Thus, even low damping coefficient of *SE* can have an important effect on the muscle model response. In the model of Figure 21, the muscle mass is determined by the element mass defined in input file.

#### Formulae for contractile element

In the current formulation of the muscle model, the muscle force is calculated with the following equations:

$$F_{Mus} = N_a(t)F_{CE}(x, v) + F_{PE}(x) + F_{DE}(v) \quad \text{and} \quad (6)$$

$$F_{CE}(x, v) = F_l(x) F_v(v), \quad (7)$$

where  $F_{Mus}$  is the total muscle force,  $N_a$  is a function which determines the muscle active state,  $F_{CE}$  is the force in the contractile element of fully activated muscle,  $F_{PE}$  is the force in the parallel elastic element,  $F_{DE}$  is the force in the parallel viscous element,  $F_l$  is the function which determines the relation between active muscle force and muscle elongation  $x$ , and  $F_v$  is the function which determines the relation between active muscle force and velocity of muscle elongation/shortening  $v$ .

Mathematical expressions for  $F_l$ ,  $F_v$ ,  $F_{PE}$  and their parameters are based on equations presented by Winters and Stark (1985, 1988) which describe muscle characteristics in terms of joint angular displacement. These equations were modified by the authors in order to express muscle behaviour in terms of muscle elongation and velocity of elongation/shortening, which is more suitable for FE modelling.

The active muscle force—length relation is calculated here with the following formula:

$$F_l(x) = F_{max} \exp \left( - \left( \frac{\frac{l}{l_{opt}} - 1}{C_{sh}} \right)^2 \right), \quad (8)$$

where  $F_{max}$  is the maximum isometric muscle force,  $l$  is the muscle fibre length,  $l_{opt}$  is the optimum length of the muscle fibre, and  $C_{sh}$  is a shape parameter which determines concavity of

the muscle force—length characteristics, see Figure 22.  $l_{opt}$  is defined as the fibre length at which generation of the muscle force is the most efficient. In the current study,  $l_{opt}$  is expressed as a ratio of the muscle fibre length at rest  $l_{fib}$ .

Force—velocity characteristics are defined here as the relation between the maximum muscle force and instantaneous rate of the muscle length change when a muscle is fully activated at its optimum length:

$$F_v(v) = \begin{cases} 0 & \text{for } v_n \leq -1 \\ \frac{1 + v_n}{1 - \frac{v_n}{C_{short}}} & \text{for } -1 < v_n \leq 0 \\ \frac{1 + v_n \frac{C_{mvl}}{C_{leng}}}{1 + \frac{v_n}{C_{leng}}} & \text{for } v_n > 0, \end{cases} \quad (9)$$

where  $v_n$  is the muscle elongation/shortening velocity normalised to the maximum shortening velocity  $v_{max}$ ,  $v_n = \frac{v}{v_{max}}$ ;  $C_{short}$  is the shape parameter for muscle shortening;  $C_{leng}$  is the shape parameter for muscle lengthening; and  $C_{mvl}$  is the parameter which determines the ratio of ultimate force during active lengthening to the isometric force at full activation, see Figure 23.

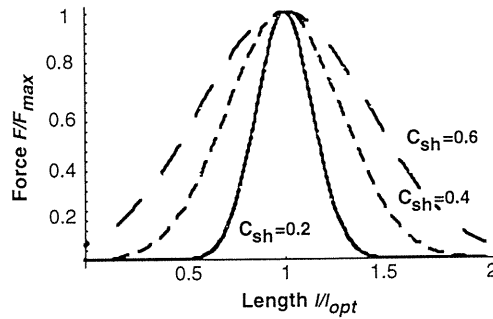


Figure 22 Active muscle force—length characteristics for different values of  $C_{sh}$ .

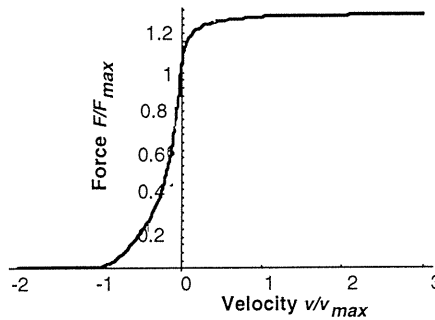


Figure 23 Active muscle force—velocity characteristic.

According to Winters and Stark (1985)  $C_{short}=0.1$  for muscles that contain high number of slow fibres, and  $C_{short}=0.5$  when the number of fast fibres is high. More accurate values for  $C_{short}$  can be obtained with the equation of Winters and Stark (1988):

$$C_{sh} = 0.1 + 0.4 C_{fast} , \quad (10)$$

where  $C_{fast}$  is the fraction of fast muscle fibres in a given muscle.  $C_{mvl}$  is usually measured to be in a range of 1.3–1.5 (Winters and Stark, 1985). Maximum shortening velocity can be calculated with the formula of Winters and Stark (1988):

$$v_{max} = 2 l_{fib} [s^{-1}] + 8 l_{fib} [s^{-1}] C_{fast} . \quad (11)$$

Simplified formulae for estimation of  $v_{max}$  were presented (Herzog, 1994) who proposed that for muscles with high number of slow fibres

$$v_{max} = 6 l_{opt} [s^{-1}] , \quad \text{and} \quad (12)$$

for muscles with high number of fast fibres

$$v_{max} = 16 l_{opt} [s^{-1}] . \quad (13)$$

#### Formulae for parallel element

In the present muscle model, force in the parallel elastic element  $F_{PE}$  is calculated with the equation of Winters and Stark (1985):

$$F_{PE} = \frac{F_{max}}{\exp(C_{PE}) - 1} \left\{ \exp \left( \frac{C_{PE}}{PE_{max}} \left( \frac{l}{l_{fib}} - 1 \right) \right) - 1 \right\} , \quad (14)$$

where  $C_{PE}$  is the shape parameter of the force—elongation characteristics of the parallel elastic element  $PE$ , and  $PE_{max}$  is the elongation of the parallel element at  $F_{max}$  expressed as a ratio of  $l_{fib}$ , see Figure 24.

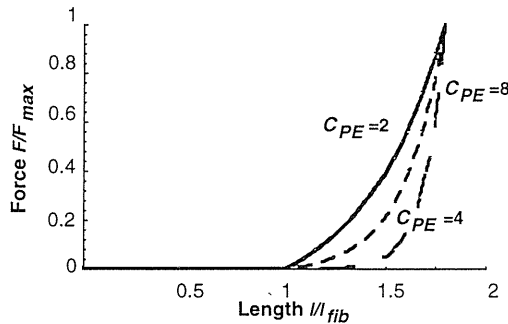


Figure 24 Passive muscle force—length characteristic.

Force in the parallel damper  $F_{DE}$  is given by the formula:

$$F_{DE} = k_{DE} v, \quad (15)$$

where  $k_{DE}$  is a damping coefficient.

#### Formulae for series elastic element/tendon

In the current formulation of the Hill-type muscle model, the series elastic element  $SE$  is interpreted as a tendon. In the literature, force—elongation curve of a tendon is usually divided in two regions: non-linear and linear (Carlstedt and Nordin, 1989, Giat et al., 1994). In the present study, the non-linear tendon force—elongation properties were calculated with an exponential relation proposed by Winters and Stark (1988). The final form of formulae for calculation the tendon force—elongation relationship is:

$$F_{SE} = \begin{cases} \frac{F_{\max}}{\exp(C_{SE}) - 1} \left\{ \exp\left(\frac{C_{SE} x_{SE}}{SE_{\max}}\right) - 1 \right\} & \text{for } x_{SE} \leq x_{\text{elast}} \\ k_{SE}(x_{SE} - x_{\text{elast}}) + F_{\text{elast}} & \text{for } x_{SE} > x_{\text{elast}} \end{cases} \quad (16)$$

where  $F_{SE}$  is the tendon force,  $x_{SE}$  is the tendon elongation,  $SE_{\max}$  is the tendon elongation at  $F_{\max}$ ,  $C_{SE}$  is the shape parameter of the tendon force—elongation characteristics,  $k_{SE}$  is the tendon linear stiffness,  $x_{\text{elast}}$  is the tendon elongation beyond which the force—elongation characteristics are linear, and  $F_{\text{elast}}$  is the tendon force at  $x_{\text{elast}}$ .  $SE_{\max}$  and  $x_{\text{elast}}$  are given as a ratio of the tendon slack length  $l_{\text{slack}}$ . The slack length is the length beyond which the tendon develops force.  $k_{SE}$  is calculated with the following equation:

$$k_{SE} = \frac{C_{SE}}{SE_{\max}} \frac{F_{\max}}{\exp(C_{SE}) - 1} \exp\left(\frac{C_{SE} x_{\text{elast}}}{SE_{\max}}\right). \quad (17)$$

From the literature data it can be estimated that  $SE_{\max}$  is about 0.03–0.05  $l_{\text{slack}}$  (Winters and Stark, 1988), and  $x_{\text{elast}}$  is about 0.01–0.02  $l_{\text{slack}}$  (Pandy et al., 1990, Giat et al., 1994). Sample results calculated with Eqs. (16)–(17) are shown in Figure 25.

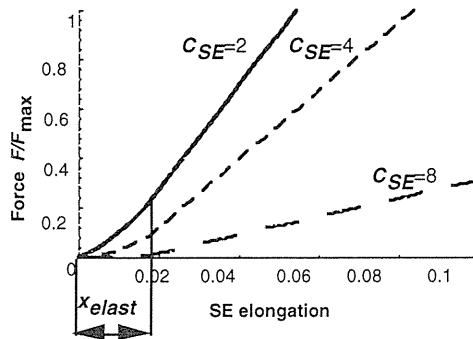


Figure 25 Tendon/SE force—elongation characteristic.

### Neural control and reflex time

Subroutines for PAM-CRASH code developed here facilitate two ways to define the time of start of the neuromuscular reaction:

1. The start time — defined as the time lag  $T_{reflex}$  between the start of simulation and the time when the neuromuscular reaction is initialised. This time lag is arbitrarily defined by the user, and the neurocontroller input signal  $u$  has the form:

$$u = \begin{cases} 0 & t \leq T_{reflex} \\ 1 & t > T_{reflex} \end{cases} \quad (18)$$

2. The start time — defined by selection of a sensitivity level of stretch receptors located in muscle spindles, which enables to model a stretch reflex. In the current study, this sensitivity level was defined as a threshold of the muscle elongation  $x_{trig}$ . With this definition the neuromuscular reaction cannot be initialised when the muscle elongation is lower than  $x_{trig}$ . Thus, the neurocontroller input signal  $u$  is

$$u = \begin{cases} 0 & x_{CE} \leq x_{trig} \text{ or } t \leq T_{reflex} \\ 1 & x_{CE} > x_{trig} \text{ and } t > T_{reflex} \end{cases} \quad (19)$$

The signal  $u$  is the input to equations which describe the dynamics of the neuromuscular excitation and the dynamics of the muscle active state. In the current study, the excitation-activation equations of Winters and Stark (1985, 1988) are used. These equations were discussed in detail in the first part of the present report, see Eqs. (3)–(4) in Chapter 1. Since in the current formulation of FE muscle model signal  $u$  was assumed to be either 1 (activated muscle) or 0 (non-activated muscle), there exists analytical solution of the excitation-activation equations:

$$N_a(t) = \begin{cases} A_{init} & \text{for } t \leq T_{reflex} \\ 1 + \frac{(A_{init} - 1)(T_a - T_{ne}) - T_{ne}}{(T_a - T_{ne}) \exp\left(\frac{t - T_{reflex}}{T_a}\right)} + \frac{T_{ne}}{(T_a - T_{ne}) \exp\left(\frac{t - T_{reflex}}{T_{ne}}\right)} & \text{for } t > T_{reflex} \end{cases} \quad (20)$$

where  $N_a$  is the muscle active state,  $A_{init}$  is initial value for the muscle active state,  $T_{ne}$  is the time constant of excitation, and  $T_a$  is the time constant of activation. When a muscle is not activated at the beginning of simulation,  $A_{init}$  equals the minimum value of the muscle active state  $A_{min}$ . According to Hatze (1981)  $A_{min}=0.005$ .  $T_a$  and  $T_{ne}$  can be calculated with the formulae proposed by Winters and Stark (1985, 1988):

$$T_{ne} = C_1 + C_2 m C_{slow} \quad (21)$$

$$T_a = B_1 + B_2 m (C_{slow})^2, \quad (22)$$

where  $T_{ne}$  and  $T_a$  are given in seconds,  $C_1=0.025$  s,  $C_2=0.010$  s,  $B_1=0.005$  s,  $B_2=0.0005$  s,

$m$  is the muscle mass in grams, and  $C_{slow}$  is the fraction of slow muscle fibres. Eqs. (21)–(22) yield values from 0.02 s to 0.05 s for  $T_{ne}$ , and values from 0.005 to 0.020 s for  $T_a$ .

### Equilibrium of muscle-tendon unit

The current formulation of FE muscle model makes it possible to calculate initial elongation of the muscle  $x_{CE}$  and the tendon  $x_{SE}$  to satisfy the static/isometric equilibrium of the muscle-tendon unit for a given initial value of the muscle active state. This requires to solve the system of two non-linear equations:

$$\begin{cases} A_{init} F_{CE}(x_{CE}, v = 0) + F_{PE}(x_{CE}) = F_{SE}(x_{SE}) \\ x_{CE} + x_{SE} = 0, \end{cases} \quad (23)$$

where  $F_{CE}$ ,  $F_{PE}$ , and  $F_{SE}$  are calculated with Eqs. (6)–(17). System of equations Eq. (23) is solved with the Newton-Raphson method (Press et al., 1992a, Press et al., 1992b).

### 2.2.2 Software implementation of finite element muscle model

All subroutines for calculation of muscle and tendon force were written in FORTRAN 77 as modules for PAM-CRASH software library. The flow chart of the subroutine that calculates muscle force is shown in Figure 26.

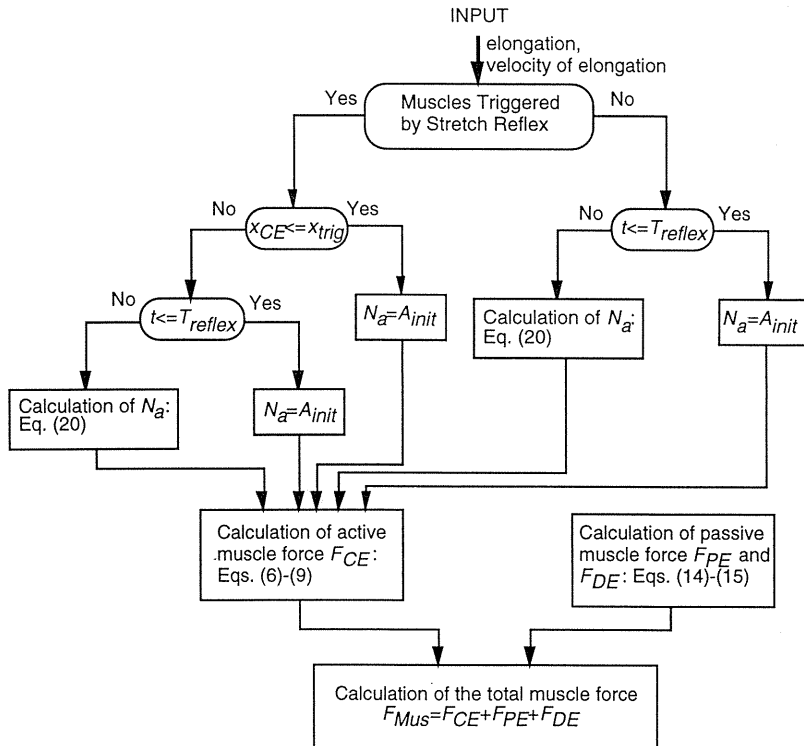
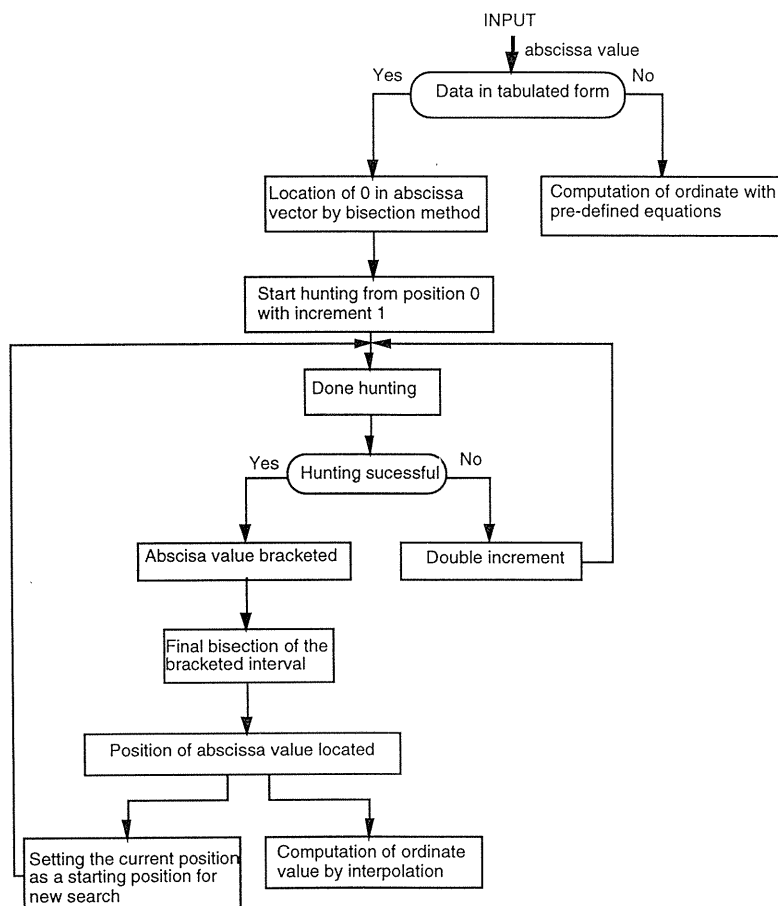


Figure 26 Flow chart of the subroutine for muscle force calculation.



**Figure 27** Flow chart of the subroutine which uses “hunting” algorithm to calculate characteristics of a muscle model from tabulated data.

All the parameters to Eqs. (8)–(20) have to be specified by the user in an input file. It should be noted here that Eqs. (8)–(20) are based on typical formulae commonly used in the literature, which may not be enough to fit specific features of given muscle behaviour under transient loads. For this reason the current software implementation of FE muscle model enables an optional input of the model characteristics in a tabular form, see Figure 27. Tabulated input data are linearly interpolated, and the “hunting” algorithm with correlated values is used to search the tables (Press et al., 1992a, Press et al., 1992b).

### 2.2.3 Model validation

The muscle model was validated by comparison of the calculated muscle force-time histories with the experimental results of muscle isometric contraction by Bahler et al. (1968) and with the results of fast lengthening of a muscle by Kirsch et al. (1994).

The experiments by Bahler et al. (1968) were performed on gracilis muscle from white



male rats. Rats were anaesthetised, and the gracilis muscle was freed from neighbouring muscles and removed together with a portion of the tibia and pubis bones. The muscle was loaded with the system consisted of a light-weight lever and an electromechanical torque source. Muscle force was measured with a cantilever transducer that was deformed by the muscle. The muscle was supramaximally stimulated by electrodes which set electric field perpendicular to the longitudinal muscle axis.

The experiments by Kirsch et al. (1994) were done on soleus muscle from anaesthetised cats. The muscle was separated from the surrounding tissue, and its distal end was attached to a force transducer. Rapid “step” stretches with a speed of up to 110.9 mm/s and amplitude of up to 1.6 mm were applied to the muscle.

In simulation of both described above experiments, the muscle-tendon unit was modelled with five elements: three elements of a muscle type and two elements of a tendon type, see Figures 28 and 29, respectively. All characteristics for the muscle and tendon models were determined with functions defined by Eqs. (8)–(17).

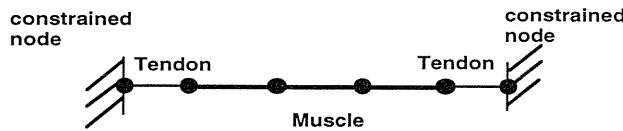


**Figure 28** Set-up of the simulation test for investigation of behaviour of the current FE muscle model during isometric contraction.

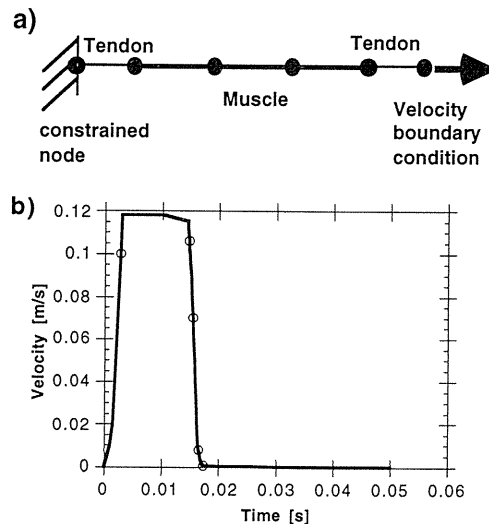


**Figure 29** (a) Set-up of the simulation test for investigation of behaviour of the current FE muscle model during “step” stretch. (b) Velocity–time curve for definition of the velocity boundary condition. The velocity curve is based on the paper by Kirsch et al. (1994).

Validation against isometric and “step” stretch tests may not be enough to prove that the current muscle model can be effectively used to analyse muscle effect on biodynamic response of the human body segments in car collisions. Therefore the authors used a simplified model of the head-neck complex in a frontal impact in order to investigate behaviours of the muscle model under more realistic conditions. The present head-neck model consists of one extensor muscle modelled with 5 finite elements and two rigid links: torso link and head-neck link, see Figure 30. Thus, the joint between the head and neck was disregarded, and the head-neck model has only one rotational degree of freedom. The current head-neck model is based on the model developed by Happee and Thunnissen (1994a), and it can be treated as a simplification of the model used in Chapter 1. Horizontal acceleration of the first thoracic vertebra  $T_1$  was used as a load of the head-neck complex, see Figure 30. The  $T_1$  acceleration pulse corresponds to a frontal impact with an initial velocity of 50 km/h and peak acceleration of 15 g. This pulse was taken from the application examples of MADYMO multibody code for crash victims simulation (TNO, 1996). In order to investigate the muscle model behaviour under different conditions of the muscle active state, the following circumstances were analysed: 1)  $A_{init}=A_{min}$  and  $T_{reflex}=0.04$  s; 2)  $A_{init}=A_{min}$  and  $T_{reflex}=0$ ; 3) Muscles relaxed during impact, i.e.  $N_a$  is constant and equals  $A_{min}$ ; and 4) Muscles triggered by the stretch reflex with  $A_{init}=A_{min}$ ,  $x_{trig}=0.05l_{opt}$ , and  $T_{reflex}=0.04$  s. So far the authors have found no relevant experimental data on the human cervical muscle force in impacts. For this reason

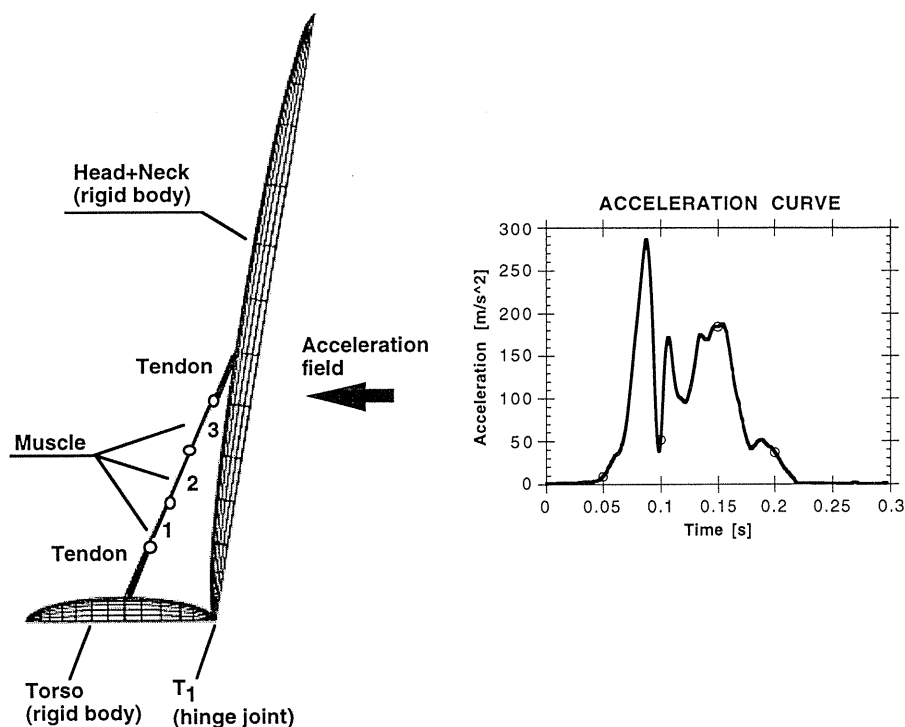


**Figure 30** Simplified model of the head-neck complex for validation of the current FE muscle model and an acceleration—time curve for simulation of an acceleration field. The curve was taken from the MADYMO manual (TNO, 1996).

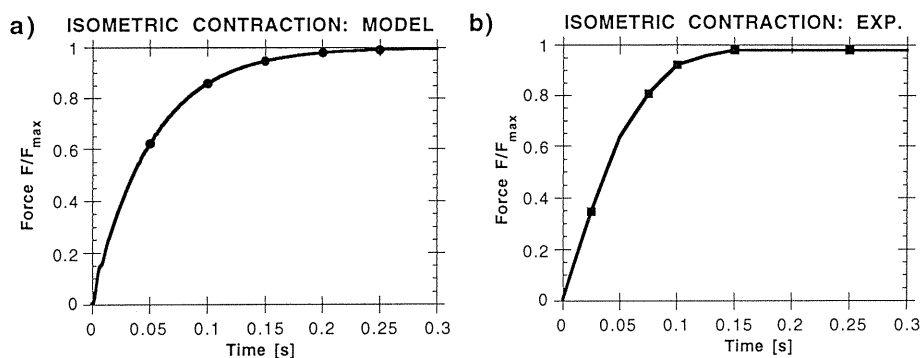
the current tendon and muscle forces-time histories were compared with the experimental results on electromyographically derived force of a dog's spinal neck muscle presented by Tennyson et al. (1977). In their experiments anaesthetised dogs were subjected to vertical acceleration of 5 g. Thus, conditions of those experiments differ from the current simulation of the frontal impact. For this reason the data by Tennyson et al. (1977) can be used only for qualitative comparison with the results calculated here. Another important limitations of the current procedure for validation of the muscle model are that it disregards the skin stiffness and contact between muscles and the skeleton, which may lead to large displacements of the muscle elements' nodes when the head-neck model is subjected to an acceleration field. Moreover, disregarding the contact between muscles and the skeleton and assuming that a skeletal muscle has a form of a straight line can result in inaccuracies when calculating the muscle elongation and moment arms of the muscle force about joints.

### 2.3 Results

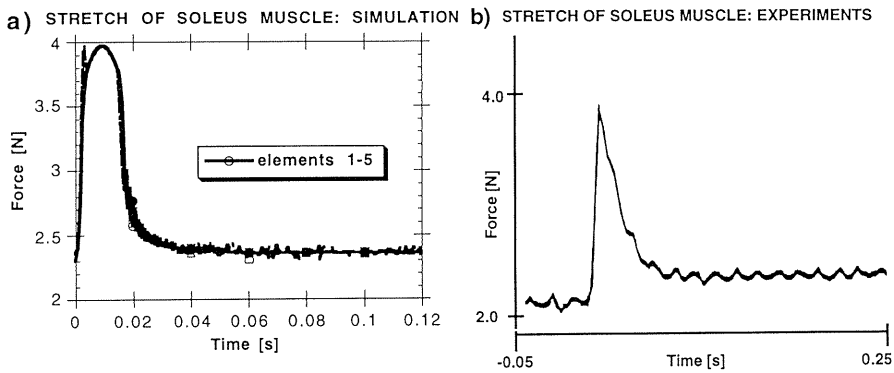
Muscle force-time histories calculated here and the experimental results by Bahler et al. (1968) are compared in Figure 31. This figure shows that the current model of a skeletal well muscle well predicted the behaviour of the rat gracilis muscle during isometric contraction with supramaximal muscle activation since the present modelling results differ from experimental data in less than 10%.

Figure 32 shows muscle force-time histories obtained in the present study and the experimental data by Kirsch et al. (1994) on muscle "step" stretch. The current model of skeletal muscle correctly predicted that an initial region where the muscle force rapidly increases is followed by the region where the force declines, and that the force after decline is never lower than the initial force level, see Figure 32. Furthermore, the calculated peak value of the muscle force was very close to the value measured by Kirsch et al. (1994). On the other hand, the current results differ from the experimental data by Kirsch et al. (1994) in three important points: 1) The present force-time curves of the muscle force decline more rapidly than in the experiments; 2) The calculated level of the muscle force after a decline is lower the one measured by Kirsch et al. (1994); and 3) The muscle model exhibits force oscillation with low amplitude and relatively high frequency, see Figure 32b.

One possible explanation for fast decline of the force can be that in the current formulation of the Hill-type model, the force-velocity characteristics were assumed to be



**Figure 31** Isometric contraction of a rat gracilis muscle. (a) Results obtained with the current muscle model. (b) Experimental curve based on Bahler et al. (1968).



**Figure 32** “Step” stretch of cat soleus muscle. **(a)** Results of the current study. **(b)** Experimental results. Adapted from Kirsch et al. (1994). Oscillations in the experimental curve are caused by stimulation of the soleus muscle with a frequency of 60 Hz.

history-independent, see Eq. (9). Thus, the force yielding phenomenon was disregarded, which may lead to inaccuracies when predicting the behaviour of cat soleus muscle during transient lengthening (Winters, 1990). Furthermore, exact data on the optimal muscle length  $l_{opt}$  of cat soleus are not available from the paper by Kirsch et al. (1994). The authors estimated the cat soleus  $l_{opt}$  from the literature data on the human muscles (Hoy et al., 1990). Such estimation introduces inaccuracies, which can affect calculation of the muscle force. High frequency oscillation of the muscle force-time histories are directly related to application of the finite element method to solve dynamics of Hill-type muscle model. Finite element Hill-type model can be considered to be a lumped-parameter system which consists of non-linear springs, dampers and nodal masses. When such a system is perturbed from its equilibrium by a rapid stretch, it oscillates according to its eigen-modes. It is also likely that oscillations of the muscle force were amplified by the force–velocity characteristics. The slope of these characteristics rapidly changes when the muscle deformation velocity crosses zero, which makes muscle force calculation very sensitive to the velocity changes.

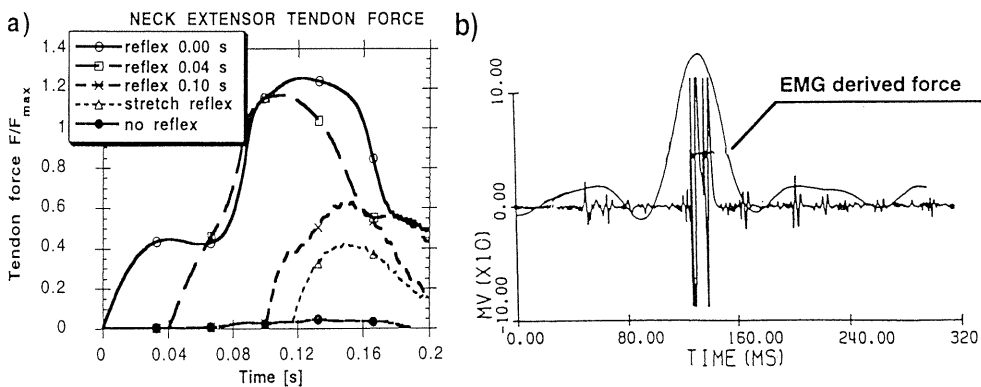


**Figure 33** **(a)** Tendon force-time histories of the neck extensor computed in the current study. **(b)** Electromyographically derived force of canine spinalis cervicis obtained by Tennyson et al. (1977).

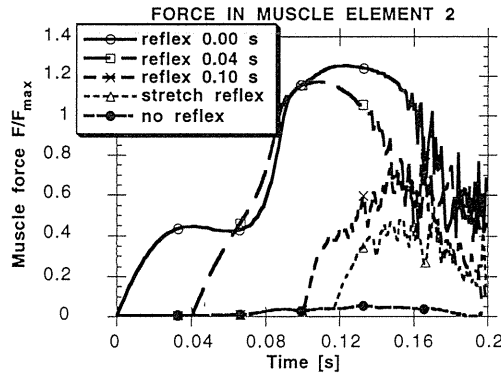


**Figure 34** Muscle force-time histories computed with the current muscle model for different reflex times.

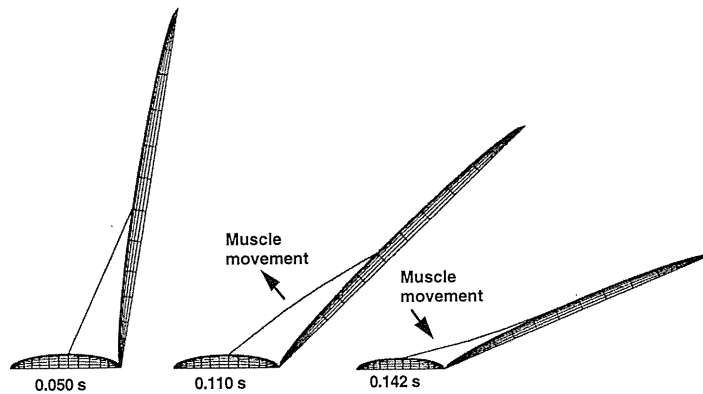


**Figure 35** Kinematic responses of a simplified model of the head-neck complex at 0.050 s, 0.110 s, and 0.142 s.

Results obtained with the simplified model of the head-neck complex indicated that the calculated tendon force-time histories correspond in form to the electromyographically derived force obtained by Tennyson et al. (1977), see Figure 33. On the other hand, the muscle force-time histories exhibited strong oscillation, see Figure 34. Amplitude of these oscillations greatly increased for long reflex times, which is similar to the effect observed for the multibody formulation of the muscle model with the lumped mass, compare Figure 13. An important factor contributing to the strong oscillation of the muscle force was “violent” forward and backward movement of the neck extensor, see Figure 35. This violent movement resulted from inertial forces. Its amplitude was high since there was no contact between muscle elements and the neck in the current head-neck structure.

## 2.4 Discussion

From the present study it can be concluded that the current muscle model gives responses close to the experimental results under both isometric contraction and transient loads conditions, see Figures 31 and 32. The model correctly predicted the rapid increase of force during transient stretch and the decline of force after the stretch. However, the calculated rate of the force decline and the force value after that decline slightly differed from the experimental data by Kirsch et al. (1994). The authors hypothesise that those differences could result from disregarding muscle force yielding phenomenon in the current muscle model.

Therefore in more detail investigation of muscle effect on the biodynamic response of the human body in car collisions may require to take into account yielding phenomenon and to modify mathematical formulae for the current finite element muscle model. Such modification can be done with the “attachment” concept of Winters (1990) who proposed to distinguish between the muscle active state and the number of attached calcium-troponin bonds. Since the number of attached bonds is proportional to the muscle capability to generate force, Winters (1990) replaced the muscle active state  $N_a$  with attachment  $A_{att}$ :

$$F_{att}(N_a, v) = F_{act}(N_a) - F_y(A, v), \text{ and} \quad (24)$$

$$F_{CE}(x, v, t) = A_{att}(t) F_l(x) F_v(v) \quad (25)$$

where  $F_{act}$  and  $F_{att}$  are activation and attachment functions, respectively;  $F_{CE}$  is the contractile element force;  $F_y$  is the yielding function;  $x$  is the muscle elongation; and  $v$  is the velocity of the muscle shortening/lengthening. Winters (1990) proposed the following formulae to calculate  $F_y$ :

$$\tau \dot{F}_y + F_y = \begin{cases} \left( \frac{v}{v_{\max}} \right)^{0.5} \left( \frac{kF_a + F_{\max}}{k + 1} \right) \left( 1 + \frac{\dot{N}_a}{\dot{N}_{a_{\max}}} \right) & v > v_{cr}, \\ 0 & v \leq v_{cr} \end{cases} \quad (26)$$

$$\tau = \frac{\tau_0}{1 + \frac{v}{v_{\max}}}, \quad (27)$$

where  $\tau$  is the time parameter of yielding function,  $\tau_0$  is the value of  $\tau$  at  $v=0$ ,  $\dot{N}_a$  is a rate of change of the muscle active state,  $\dot{N}_{a_{\max}}$  is the maximum rate of change of the muscle active state,  $k$  is a constant, and  $v_{cr}$  is the critical velocity of muscle lengthening which determines the yielding point. While simulating muscle force yielding, Eqs. (26)–(27) should be combined with Eqs. (18)–(20). In consequence, the order of the muscle model increases. For this reason, the authors propose to perform a parameter study of Eqs. (26)–(27) in order to investigate how much these equations affect the computation time and complexity of the muscle model. Results calculated with the simplified finite element model of the head-neck complex in a frontal impact showed that force-time histories of the neck extensor tendon well correspond in form to the electromyographically derived force obtained by Tennyson et al. (1977) and to the results computed with the multibody model of skeletal muscle presented in Chapter 1, see Figure 33 and 36. Therefore it can be concluded that the current finite element model of a skeletal muscle yields, at least, reasonable responses under impact conditions.

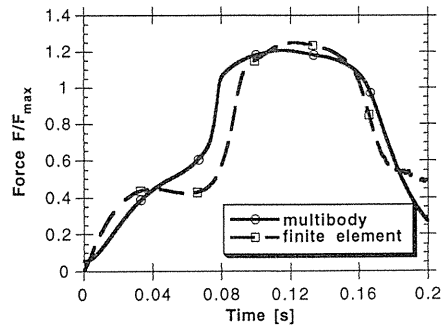


**Figure 36** Comparison of the neck force-time histories calculated with the multibody and finite element formulations for the muscle model. Figures shows results for tendon type finite elements only.

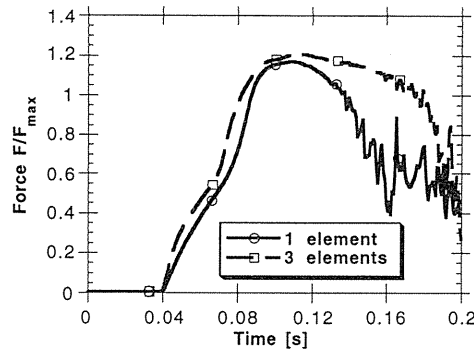


**Figure 37** Comparison of the neck extensor force-time histories calculated with the models which consist of only one and three elements of muscle type.

The disadvantage of the current formulation for finite element muscle model is that it led to strong oscillations of the force in finite elements of a muscle type. As it has been already mentioned in the results section, there are three factors which cause these oscillations. The first factor is that the current extensor model consists of five finite elements which can vibrate according to their eigen-modes when they are perturbed from their equilibrium by rapid movements of the head-neck model in the acceleration field of a frontal collision. Accordingly, oscillation of the muscle force strongly decreased when the extensor muscle was simulated with only one finite element of a Hill-type, see Figure 37.

The second factor which contributed to the muscle force oscillation is a force—velocity relationship. For the current muscle force—velocity characteristics, the change of the muscle lengthening velocity from  $0.5v_{max}$  to  $-0.5v_{max}$  results in decrease of the muscle force from about 1.2 to 0.3, see Figure 38a. Therefore even a small variation of the muscle deformation

velocity from lengthening to shortening strongly affects the muscle force magnitude. A direct evidence that muscle force—velocity characteristics are an important cause of the current muscle force oscillations is presented in Figure 38b. This figure shows that oscillations of the muscle force were greatly decreased when the force—velocity characteristic was simplified with a constant value 1, *i.e.*  $F_v(v)=1$ .

The third cause of the neck extensor force oscillations observed here is that kinematic responses of the current model of the head-neck complex exhibited violent movements of the muscle elements' nodes, see Figure 35. These movements resulted from inertial forces. Large movements of skeletal muscles and internal organs are observed when volunteers and cadavers are subjected to an acceleration field, *e.g.* Schröder (1997). Since there was no contact between muscles and skeleton in the current model of the head-neck complex, and the skin stiffness was disregarded, the movements' amplitude was higher than the one observed in the experiments.

It should be noted that oscillations of the muscle force discussed here can only slightly influence results of mathematical modelling of muscle effects on kinematic responses of the human body in a car collision. Results of such modelling primarily depend on calculation of the tendon forces which directly act on the human body segments. Figure 33 shows that the current tendon force-time histories yield relevant results. However, elimination or decreasing oscillations of the muscle force can still improve biofidelity of the current model responses.

The problem is that not all of three discussed above factors which cause these oscillations can be completely removed. For instance, the muscle model which consists of only one finite element does not oscillate, see Figure 37. However, such a simplified model has important limitations. It disregards tendon, which may lead to inaccuracies in calculation of the muscle force-time histories, see Figure 12. Model of a whole muscle-tendon unit requires to use, at least, three finite elements: two elements of a tendon type and one element of a muscle type. Furthermore, several finite elements may be necessary to fit curved shapes of muscles' force action lines. Simplification of a complex shape of the muscle force-velocity characteristics as constant value greatly smoothed the calculated muscle force-time histories, see Figure 38b. However, such simplification can cause strong inaccuracies when calculating muscle force

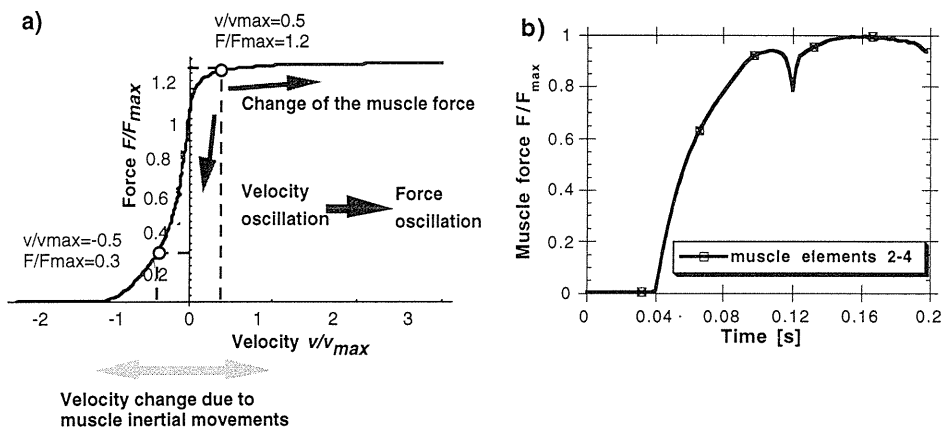


**Figure 38** (a) Muscle force—velocity characteristics. Small change of the muscle velocity from shortening to lengthening can lead to large changes of the muscle force. (b) Muscle force-time histories calculated with the force—velocity characteristics simplified as a constant value equalled 1, *i.e.*  $F_v(v)=1$ .



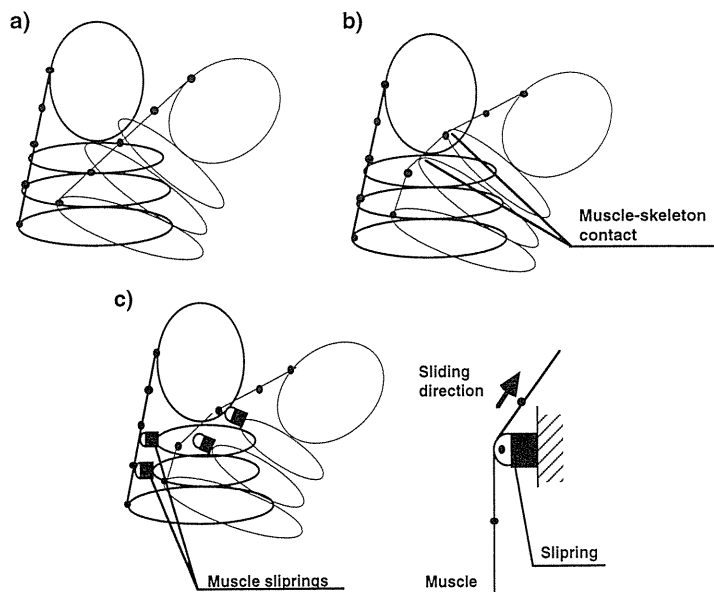


**Figure 39** (a) Scheme of kinematic response of the current muscle model. (b) Desired response of the model in which a contact between muscle and skeleton is taken into account. (c) Determining a muscle action line by slippings.

under transient muscle loads. Therefore the optimal method to minimise oscillations of the muscle force is to decrease amplitude of violent movements of the muscle elements' nodes in an acceleration field. This can be done in two alternative ways: 1) Modelling of contact between muscles and the skeleton, or 2) Application of slippings in order to allow muscles to slip on joints' surfaces. Furthermore, both of them enable to accurately predict a muscle moment arm and a muscle force action line, which is necessary for in-depth analysis of the muscle effect on biodynamic responses of the human body in car collisions, see Figure 39.

Natural way to model contact between muscle and the skeleton is to apply two-dimensional or three-dimensional muscle elements instead of the current one-dimensional fibre model. Furthermore, shell or solid muscle models are required for modelling of structural responses of skeletal muscles. Such models can be developed in PAM-CRASH based on the current implementation of the Hill-type muscle model.

Application of slippings would require less effort than development of new two- or three-dimensional muscle models since they are available in PAM-CRASH as a standard entity for modelling seat-belts. One possible disadvantage of such solution is that slippings may introduce a small amount of numerical oscillations to the muscle force (ESI, 1996). These oscillations will be added to the muscle force oscillations reported in the present study, which may negatively affect responses of the muscle model.

In summary, it can be concluded that the current one-dimensional muscle model in PAM-CRASH is suitable for modelling basic features of skeletal muscle behaviour under both isometric and transient load conditions. For improvement of biofidelity and efficiency of this model, it is recommended to perform its further development to model contact between

muscles and the skeleton. A direct way for such development is to apply two-dimensional or three-dimensional muscle elements instead of the current one-dimensional fibre model.

### Summary

The parameter study of the muscle effect on the head-neck complex kinematics described in Chapter 1 indicated that muscles can significantly affect the head-neck complex kinematics in a frontal impact when the following two conditions are satisfied simultaneously: 1) Peak of horizontal acceleration of the first thoracic vertebra is less than 70 g, and 2) Reflex time is lower than 60 (80) ms. The calculated muscle effect was not sensitive neither to a structure nor to the most parameters of the Hill-type muscle models. Some differences in responses were found only between the models with a series elastic element and without this element. Tendency of the results obtained with the present head-neck model well agreed with the experimental literature. However, the current simplification of the head-neck complex as two rigid links and simplification of muscles as one-dimensional actuators with point mass are deficient for in-depth analysis of the muscle effect on the head-neck complex kinematics. Such analysis requires to accurately model the head-neck complex geometry, which can be done by finite element analysis.

Since commercial finite element codes do not enable to model skeletal muscles, the authors implemented a new Hill-type muscle model in PAM-CRASH code. A structure of this model was selected based on the results of the parameter study. Validation of the current finite element muscle model indicated that this model captures essential behaviours of a skeletal muscle under both isometric contraction and transient loads conditions. Therefore this model can be used as the basis for further development of two- and three-dimensional finite element muscle models which are recommended here for an in-depth analysis of muscle effect on the biodynamic responses of the human body in car collisions.

### Acknowledgements

The parameter study of the muscle effect on the head-neck complex kinematics described in Chapter 1 was begun at the Department of Injury Prevention at Chalmers University of Technology in Gothenburg, Sweden, and it was completed at the Human Life Support Biomechanics Laboratory at the Nagoya University, Japan. Development of the finite element muscle model described in Chapter 2 was done at the Human Life Support Biomechanics Laboratory of Nagoya University in cooperation with PAM System International (PSI) from Rungis, France and Nihon PSI from Tokyo.

The authors thank all those who supported us in this study, and in particular:

Professor Roland Örtengren, head of the Department of Injury Prevention, Chalmers University of Technology, for valuable discussion and advices;

Doctor David Viano, guest professor at the Department of Injury Prevention, for his constructive criticism and valuable comments;

Professor Krzysztof Kędzior, head of the Institute of Aeronautics and Applied Mechanics of Warsaw University of Technology, Poland, for his valuable advices;

Doctor Eberhard Haug, scientific director of Engineering System International, Rungis, France, for his valuable comments and cooperation in development of muscle model in

PAM-CRASH code;

Doctor Xiaomin Ni, PAM-CRASH general software manager, for his help in software implementation of muscle model in PAM-CRASH code.

## Appendix 1: Dynamics of the head-neck model

### Nomenclature

$\theta_1$ = lower joint angle	$M_{load2}$ = torque from external load about the upper joint
$\theta_2$ = upper joint angle	$M_{ei1}$ = torque from the extensor $i$ about the lower joint
$g$ = gravity acceleration	$M_{fi1}$ = torque from the flexor $i$ about the lower joint
$m_1$ = neck mass	$ne_1$ = number of extensors acting on the lower joint
$m_2$ = head mass	$nf_1$ = number of flexors acting on the lower joint
$I_1$ = moment of inertia of the neck about the neck center of mass	$M_{ei2}$ = torque from extensor $i$ about the upper joint
$I_2$ = moment of inertia of the head about the head center of mass	$M_{fi2}$ = torque from flexor $i$ about the upper joint
$a_1$ = coordinate of the neck center of mass	$ne_2$ = number of extensors acting on the upper joint
$a_2$ = coordinate of the head center of mass	$nf_2$ = number of flexors acting on the upper joint
$l_1$ = neck length	
$M_{T1}$ = passive resistive joint torque about the lower joint	
$M_{occ}$ = passive resistive joint torque about the upper joint	
$c_1$ = damping coefficient of lower joint	
$c_2$ = damping coefficient of upper joint	
$M_{load1}$ = torque from external load about the lower joint	

### Dynamics of the head-neck model

The current head-neck model is a 2-D model which consists of two rigid links connected by two hinge joints, see Figure 1 and Figure 1A. Equations of motion of this model are:

$$\begin{aligned}
 & \ddot{\theta}_1 (I_1 + m_1 a_1^2 + m_2 l_1^2 + 2m_2 l_1 a_2 \cos \theta_2 + I_2 + m_2 a_2^2) \\
 & + \ddot{\theta}_2 (m_2 l_1 a_2 \cos \theta_2 + I_2 + m_2 a_2^2) - (2\dot{\theta}_1 \dot{\theta}_2 + \dot{\theta}_2^2) (m_2 l_1 a_2 \sin \theta_2) \\
 & - [m_1 a_1 \sin \theta_1 + m_2 l_1 \sin \theta_1 + m_2 a_2 \sin(\theta_1 + \theta_2)] g \\
 & = M_{load1} - \sum_{ei_1=1}^{ne_1} M_{ei_1} + \sum_{fi_1=1}^{nf_1} M_{fi_1} - M_{T1} - c\dot{\theta}_1
 \end{aligned} \tag{A1}$$

and

$$\begin{aligned}
 & \ddot{\theta}_1 (I_2 + m_2 a_2^2 + m_2 l_1 a_2 \cos \theta_2) + \ddot{\theta}_2 (I_2 + m_2 a_2^2) + \dot{\theta}_1^2 (m_2 l_1 a_2 \sin \theta_2) \\
 & - m_2 a_2 \sin(\theta_1 + \theta_2) g = M_{load2} - \sum_{ei_2=1}^{ne_2} M_{ei_2} + \sum_{fi_2=1}^{nf_2} M_{fi_2} - M_{occ} - c_2 \dot{\theta}_2.
 \end{aligned} \tag{A2}$$

Body-segmental parameters of Eqs. (A1–A2) are shown in Table 1A.

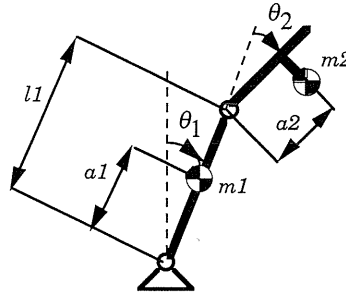


**Figure 1A** Head-neck model described by Eq. (A1) and Eq. (A2).

**Table 1A** Body-segmental parameters used in the current study.

Parameter	Value
$I_1$ [kgm <sup>2</sup> ]	0.010
$I_2$ [kgm <sup>2</sup> ]	0.029
$m_1$ [kg]	1.200
$m_2$ [kg]	4.310
$a_1$ [m]	0.060
$a_2$ [m]	0.055
$l_1$ [m]	0.130

## Appendix 2: Dynamics of the muscle models

In all the muscle models used in the present study the length of the muscle tendon unit  $l$  was calculated as a function of a given joint angle:

$$l(\theta) = l_0 + \theta r \quad (\text{A2.1})$$

where  $l_0$  is the length of the muscle-tendon unit at rest,  $q$  is a joint angle, and  $r$  is the muscle moment arm about a given joint. The lengths  $l_0$  for the muscle elements were estimated from the data of Yamaguchi *et al.* (1990). They are summarised in Table 2A.

**Table 2A** Geometrical data for the muscle elements used in the current study.

Muscle element	Muscle-tendon unit length $l_0$ [m]	Muscle fibre length [m]	Tendon length [m]
1	0.15	0.10	0.05
2	0.06	0.04	0.02
3	0.18	0.13	0.05
4	0.15	0.10	0.05
5	0.06	0.04	0.02
6	0.18	0.13	0.05

**Structure A – model without series elastic element**

The model without series elastic element is described with the following equations:

$$F_{Mus}(x, v, t) = F_{CE}(x, v, t) + F_{PE}(x) \quad (A2.2)$$

$$F_{CE}(x, v, t) = N_a(t) F_l(x) F_v(v) \quad (A2.3)$$

where  $F_{Mus}$  is the total muscle force,  $F_{CE}$  is the force in the contractile element, *i.e.* active force,  $F_{PE}$  is the force in the parallel element, *i.e.* passive force,  $N_a$  is the muscle active state of Eq. (2),  $F_l$  is the function which describes the relation between active muscle force and muscle elongation,  $F_v$  is the function which describes the relation between active muscle force and muscle shortening/lengthening velocity,  $x$  is the muscle elongation, and  $v$  is the velocity of the muscle shortening/lengthening. Mathematical expressions for  $F_l$ ,  $F_v$ ,  $F_{PE}$  and their parameters are based on the studies by Winters and Stark (1985, 1988):

- Active muscle force—elongation characteristics

$$F_l(x) = F_{max} \left\{ \exp \left( - \left( \frac{x - x_{max}}{C_{sh}} \right)^2 \right) \right\} \quad (A2.4)$$

where  $x_{max}$  is the muscle elongation at maximum isometric force,  $C_{sh}$  is the shape parameter, and  $F_{max}$  is the maximum isometric force of the muscle;

- Active muscle force—velocity characteristics

$$F_v(v) = \begin{cases} F_v(v) = 0 & \text{for } v_n < 0 \\ F_v(v) = \frac{1 + v_n}{1 - \frac{v_n}{C_{short}}} & \text{for } -1 < v_n \leq 0 \\ F_v(v) = \frac{1 + v_n \frac{C_{mvl}}{C_{leng}}}{1 + \frac{v_n}{C_{leng}}} & \text{for } v_n > 0 \end{cases} \quad (A2.5)$$

where  $v_n$  is the muscle shortening/lengthening velocity normalised to the maximum shortening velocity  $v_{max}$ ,  $v_n = \frac{v}{v_{max}}$ ,  $C_{short}$  is the shape parameter for muscle shortening,  $C_{leng}$  is the shape parameter for muscle lengthening, and  $C_{mvl}$  is the parameter which determines the ratio of ultimate force during active lengthening to the isometric force at full activation;

- Passive muscle force—elongation characteristics

$$F_{PE}(x) = \frac{F_{max}}{\exp(C_{PE})} \left\{ \exp \left( \frac{C_{PE}}{PE_{max}} x \right) - 1 \right\}, \quad (A2.6)$$

where  $C_{PE}$  is the shape coefficient for passive muscle force and  $PE_{max}$  is the parameter describing muscle elongation inducing passive force equal to  $F_{max}$ .

### Structure B – model with the single series elastic element

Mathematical formulae for dynamic behaviour of the model with a single series elastic element are based on the studies by Pandy *et al.* (1990) and Fung (1993). In the current model, the pennation angle was neglected. Muscle force is sum of the active and passive force

$$F_{Mus} = F_{CE} + F_{PE} \quad \text{and} \quad (A2.7)$$

$$F_{CE}(x_{CE}, v_{CE}, t) = F_{SE}(x_{SE}), \quad (A2.8)$$

where  $F_{SE}$  is the force in the series elastic element and  $x_{SE}$  is the elongation of the series elastic element,  $x_{CE}$  is the elongation of the contractile element,  $v_{SE}$  is the velocity of the series elastic element, and  $v_{CE}$  is the velocity of shortening/lengthening of the contractile element.

Based on Eqs. (A2.8) and (A2.9) the first time derivative of muscle force can be expressed as

$$\frac{dF_{Mus}}{dt} = \frac{dF_{SE}}{dt} + \frac{dF_{PE}}{dt} = k_{SE}v_{SE} + k_{PE}v_{Mus} \quad (A2.9)$$

where  $k_{PE}$  is the stiffness of the parallel elastic element and  $k_{SE}$  is the stiffness of the series elastic element. In the current study, it was assumed that the stiffness of the series elastic element and the stiffness of the parallel element are linear functions of force (Winters and Stark, 1988; Fung, 1993), which yields

$$k_{PE}(F_{PE}) = \frac{C_{PE}}{PE_{max}} F_{PE} + F_{max} \frac{C_{PE} / PE_{max}}{\exp(C_{PE}) - 1} \quad \text{and} \quad (A2.10)$$

$$k_{SE}(F_{SE}) = \frac{C_{SE}}{SE_{max}} F_{SE} + F_{max} \frac{C_{SE} / SE_{max}}{\exp(C_{SE}) - 1} \quad (A2.11)$$

where  $C_{PE}$  is the shape parameter of passive force,  $C_{SE}$  is the shape parameter of force in the series elastic element,  $PE_{max}$  is the elongation of the parallel element at  $F_{max}$ , and  $SE_{max}$  is the elongation of the series elastic element at  $F_{max}$ . Muscle elongation  $x_{Mus}$  is a sum of elongations of the series elastic element  $x_{SE}$  and the contractile elements  $x_{CE}$ , which yields

$$x_{Mus} = x_{SE} + x_{CE} \quad (A2.12)$$

$$v_{Mus} = v_{CE} + v_{SE}, \quad \text{and} \quad (A2.13)$$

$$v_{SE} = v_{Mus} - v_{CE}. \quad (A2.14)$$

Velocity of the contractile element is calculated with the following formulae:

$$F_v(v_{CE}) = \frac{F_{CE}(x_{CE}, v_{CE}, t)}{N_a(t) F_x(x_{CE})} = \frac{F_{SE}(x_{SE})}{N_a(t) F_x(x_{CE})} \quad (A2.15)$$

$$v_{CE} = F_v^{-1}(v_{CE}) \quad (A2.16)$$

Finally, dynamic equation of the muscle model with the single series elastic element are

$$\frac{dF_{Mus}}{dt} = k_{SE}(v_{Mus} - v_{CE}) + k_{PE}v_{Mus} \quad (A2.17)$$

### Structure C – model with separated series elastic element of the muscle and the tendon

The model presented here is based on the study by Pandy *et al.* (1990). The author simplified the concepts by Pandy *et al.* (1990) by neglectation of the pennation angle. Derivation of dynamic equations for this model does not qualitatively differ from the model with single series elastic element. Elongation of the whole muscle-tendon unit  $x_{MT}$  is the sum of the muscle elongation  $x_{Mus}$  and the tendon elongation  $x_T$ :

$$x_{MT} = x_{Mus} + x_T = x_{SE} + x_{CE} + x_T. \quad (A2.18)$$

The next step in derivation of dynamic equations is to take into account that

$$F_T = F_{Mus}, \quad (A2.19)$$

where  $F_T$  is the tendon force. Then the scheme which was applied to derive Eqs. (A2.6–A2.16) can be used. The final form of dynamic equations of the muscle model with tendon is:

$$\frac{dF_T}{dt} = \frac{k_T(k_{SE} + k_{PE})}{k_T + k_{SE} + k_{PE}} \left( v_{MT} - \frac{k_{SE}}{k_{PE} + k_{SE}} v_{CE} \right) \quad (A2.20)$$

where  $k_T$  is the tendon stiffness.

### Structure D – model with the muscle mass

The model presented here is based on the studies by Giat *et al.* (1994) and Shue (1995). This model can be regarded to be a modification of Hill classical model by implementing the muscle mass. The model with mass is described with the following equations:

$$F_{CE} + F_{PE} + F_{DE} + M\ddot{x}_{Mus} = F_T \quad (A2.21)$$

$$x_{MT} = x_{Mus} + x_T \quad (A2.22)$$

where  $F_{DE}$  is passive viscous force,  $M$  is the muscle mass,  $\ddot{x}_{Mus}$  is the second time derivative of the muscle elongation. Passive viscous force plays important role in this model, because it damps oscillations caused by the muscle mass. Passive viscous force equals

$$F_{DE} = k_{DE}\dot{x}_{Mus} \quad (A2.23)$$

where  $k_{DE}$  is damping coefficient of the muscle.  $k_{DE}$  was selected to be  $50 \text{ Nsm}^{-1}$  which is a value based on the studies by Schneck (1992) and Giat *et al.* (1994).

### Structure E – “black box” model

This model is based on the assumption that a muscle can be treated as a dynamic system of the second order (Dabrowska and Kedzior, 1983; Kedzior and Lackowski, 1992):

$$\tau^2 \frac{d^2 F(t)_{Mus}}{dt^2} + 2\tau \frac{dF(t)_{Mus}}{dt} + F(t)_{Mus} = u(t) F_l(x) F_v(v) + F_{PE}(x), \quad (\text{A2.24})$$

where  $t$  is time constant of the muscle and  $u(t)$  is interpreted as a dimensionless coefficient of the muscle activation  $0 \leq u \leq 1$ . When  $u=0$  the muscle is not activated, when  $u=1$  the muscle is fully activated.  $t$  was selected to be 0.025 s.

### References

- Audu, M. L. and Davy, D. T. (1985). The influence of muscle model complexity in musculoskeletal motion modeling. *Journal of Biomechanical Engineering*, **107**, 147–157.
- Bahler, A. S., Fales, J. T. and Zierler, K. L. (1968) The dynamic properties of mammalian skeletal muscle. *The Journal of General Physiology*, **51**, 369–384.
- Bowman, B. M. and Robbins, D. H. (1972). *Parameter study of biomechanical quantities in analytical neck models*. Proc. of the 16th Stapp Car Crash Conference, Wayne State University, USA. Society of Automotive Engineers, 14–43.
- Bowman, B. M., Schneider, L. W., Lustick, L. S., Anderson, W. R. and Thomas, D. J. (1984). *Simulation analysis of head and neck dynamic response*. Proc. of the International Conference on Biomechanics of Impacts (IRCOBI), Delft, The Netherlands, 173–205.
- Cailliet, R. (1981) *Neck and Arm Pain*, F.A. Davis Company, Philadelphia, USA.
- Carlstedt, C. A. and Nordin, M. (1989) Biomechanics of tendons and ligaments. *Basic Biomechanics of the Musculoskeletal System*, Edited by M. Nordin and V.H. Frankel, Lea & Febiger, 59–74.
- Dekker, M. (1988) *Finite Element Analysis*. Ed. J.R. Brauer, CAD Comp Inc.
- Dabrowska, A. and Kedzior, K. (1985). *Investigation of and modeling of the relationship between integrated surface EMG and muscle tension*. Proc. of the 9th International Congress of Biomechanics, IX-A, Edited by Winter, D. A., Waterloo, Canada, Human Kinetics Publishers, 308–312.
- ESI (1996). *PAM-SYSTEM: Programs in Applied Mechanics. Reference Manual*. PAM System International, ESI Group Software Company, Rungis, France.
- Fredriksson, L. A. (1996) *A Finite Element Data Base For Occupant Substitutes*. PhD thesis. Department of Mechanical Engineering Linköping University, Linköping, Sweden.
- Fung, Y. C. (1993). Skeletal muscle. *Biomechanics. Mechanical Properties of Living Tissues*. Springer-Verlag, New York, 392–426.
- Giat, Y., Mizrahi, J., Levine, W. S. and Chen, J. (1994). Simulation of distal tendon transfer of the biceps brachii and the brachialis muscles. *Journal of Biomechanics*, **27**, 1005–1014.
- Hallquist, J. O., Stillman, D. W. and Lin, T.-L. (1992). *LS-DYNA3D, User's Manual (Nonlinear Dynamic Analysis of Structures in Three Dimensions)*. Livermore Software Technology Corporation, USA.
- Happee, R. and Thunnissen, J. G. M. (1994a). *Advances in human body modelling using MADYMO*. Proc. of the 5th International Conference MADYMO User's Meeting, Ft. Lauderdale, Florida, USA. TNO Road Vehicles Research Institute Crash-Safety Center, Delft, The Netherlands.
- Happee, R. and Thunnissen, J. G. M. (1994b) *The Role of Muscular Dynamics in Impact Conditions, Simulation of the Head/Neck Behaviour in Frontal Car Crashes*, Report, TNO Road-Vehicles Research Institute Crash-Safety Center, Delft, The Netherlands.
- Hatze, H. (1977). A myocybernetic control model of skeletal muscle. *Biological Cybernetics*, **25**, 103–119.



- Hatze, H. (1981). *Myocybernetic Control Models of Skeletal Muscle. Characteristics and Applications*. University of South Africa, Pretoria, South Africa.
- Herzog, W. (1994). Muscle. *Biomechanics of the Musculo-Skeletal System*, Edited by B. M. Nigg and W. Herzog, John Wiley & Sons, 154–187.
- Hill, A. V. (1938). The heat of shortening and the dynamic constants of muscle. *Proceedings of Royal Society*, **126B**, 136–195.
- Hill, A. V. (1970). *First and Last Experiments in Muscle Mechanics*. Cambridge University Press, Cambridge, Great Britain, 1–77.
- Hoy, M. G., Zajac, F. E. and Gordon, M. E. (1990) A musculoskeletal model of the human lower extremity: the effect of muscle, tendon, and moment arm on the moment-angle relationship of musculotendon actuators at the hip, knee, and ankle. *Journal of Biomechanics*, **23**, 157–169.
- Huxley, A. F. (1957) Muscle structure and theories of contraction. *Progr. Biophys. Chem.*, **7**, 225–318.
- Huxley, H. and Hanson, J. (1954). Changes in the cross-striations of muscle during contraction and stretch and their structural interpretation. *Nature*, **173**, 973–976.
- Huxley, H. E. (1969). The mechanism of muscular contraction. *Science*, **164**, 1356–1366.
- Huxley, A. F. and Simmons, R. M. (1971). Proposed mechanism of force generation in striated muscle. *Nature*, **233**(:22), 533–538.
- Huyghe, J. M., Van Campen, D. H., Arts, T. and Heethaar, R. M. (1991a). The constitutive behaviour of passive heart muscle tissue: a quasi-linear viscoelastic formulation. *Journal of Biomechanics*, **24**, 841–849.
- Huyghe, J. M., Van Campen, D. H., Arts, T. and Heethaar, R. M. (1991b). A two-phase finite element model of the diastolic left ventricle. *Journal of Biomechanics*, **24**, 527–538.
- Kapandji, I. A. (1974) *The Physiology of the Joints*, Churchill Livingstone, London, Great Britain.
- Kedzior, K. and Lackowski, J. (1992). *Simulation model of a skeletal muscle*. Proceedings of the Medical Biomechanics of Spine Theory, Modelling and Clinical Application, Edited by M. Dietrich, International Centre of Biocybernetics, Podkowa Lesna, Poland. 97–108.
- Keiper, J. (1992). *Numerical computation I*. Proc. of the *Mathematica* Conference, Boston, Massachusetts, USA. Wolfram Research, 1–73.
- Lehman, S. L. (1990). Input identification depends on model complexity. *Multiple Muscle System. Biomechanics and Movement Organization*, Edited by J.M. Winters and S.L.-Y. Woo, Springer Verlag, New York, USA, 94–101.
- Ma, S. and Zahalak, G. I. (1991). A distribution-moment model of energetics in skeletal muscle. *Journal of Biomechanics*, **24**, 21–35.
- Mayoux-Benhamou, M. A., Wybier, M. and Revel, M. (1989). Strength and cross-sectional area of the dorsal neck muscles. *Ergonomics*, **32**, 513–518.
- Mecalog (1994). *RADIOSS Users' Manual*, Paris, France
- Mertz, H. J. and Patrick, L. M. (1967). *Investigation of the kinematics and kinetics of whiplash*. Proc. of the 11th Stapp Car Crash Conference, Anaheim, California, USA. Society of Automotive Engineers, 269–317.
- Mertz, H. J. and Patrick, L. M. (1971). *Strength and response of the human neck*. Proc. of the 15th Stapp Car Crash Conference, San Diego, California. Society of Automotive Engineers, 207–255.
- Morehouse, L. E. (1959). The strength of the man. *Human Factors*, **1**.
- Morgan, D. L. (1977) Separation of active and passive components of short-range stiffness of muscle. *American Journal of Physiology. Cell Physiology*, **232**, C45–C49.
- Pandy, M. G., Zajac, F. E., Sim, E. and Levine, W. S. (1990). An optimal control model for maximum-height human jumping. *Journal of Biomechanics*, **23**, 1185–1198.
- Pitman, M. I. and Peterson, L. (1989). Biomechanics of skeletal muscle. *Basic Biomechanics of the Musculoskeletal System*, Edited by M. Frankel, and V.H. Nordin, Lea & Febiger, London, Great Britain, 89–113.
- Pontius, U. R. and Liu, Y. K. (1976). *Neuromuscular cervical spine model for whiplash*. Proc. of the Mathematical Modelling Biodynamic Response to Impact, Dearborn, Michigan, USA, Society of Automotive Engineers.
- Press, W. H., Teukolsky, S. A., Vetterling, W. T. and Flannery, B. P. (1992a) *Numerical Recipes in FORTRAN: The Art of Scientific Computation*, Cambridge University Press, Cambridge, USA.

- Press, W. H., Teukolsky, S. A., Vetterling, W. T. and Flannery, B. P. (1992b) *Numerical Recipes: Example Book (FORTRAN)*, Cambridge University Press, Cambridge, USA.
- Schneck, D. J. (1992). *Mechanics of Muscle*, New York University Press, New York, USA.
- Schröder (1997), Hannover Medical School, Germany. Personal communication.
- Shue, G.-H. (1995) *System Model of Skeletal Muscle*, PhD thesis, Case Western Reserve University, Cleveland, Ohio, USA.
- Szabo, T. J. and Welcher, J. B. (1996). *Human subject kinematics and electromyographic activity during low speed rear impacts*. Proc. of the 40th Stapp Car Crash Conference, Albuquerque, New Mexico, USA, Society of Automotive Engineers, 295–315.
- Taber, L. A. (1991a). On a nonlinear theory for muscle shells: part I-theoretical development. *Journal of Biomechanical Engineering*, **113**, 56–62.
- Taber, L. A. (1991b). On a nonlinear theory for muscle shells: part II-application to the beating left ventricle. *Journal of Biomechanical Engineering*, **113**, 63–71.
- Tennyson, S. A. and King, A. I. (1976). *A biodynamic model of the human spinal column*. Proc. of the SAE Mathematical Modeling Biodynamic Response to Impact, Society of Automotive Engineers, Dearborn, Michigan, USA, 31–44.
- TNO (1996). *MADYMO: Applications Manual Version 5.2*, TNO Road-Vehicles Research Institute Crash-Safety Center, Delft, The Netherlands, 75–80.
- Verriest, J., Onser, F. M. and Viviani, P. (1975) *Changes in the dynamic behaviour of the baboon's head and neck system subjected to a frontal deceleration (-G<sub>x</sub>), related to the action of cervical muscles*. Proc. of the 2nd International Conference Biomechanics of Serious Trauma, International Research Committee on the Biokinetics of Impacts, Birmingham, Great Britain, 207–219.
- Williams, J. L. and Belytschko, T. B. (1983). A three-dimensional model of the human cervical spine for impact simulation. *Journal of Biomechanical Engineering*, **105**, 321–331.
- Winters, J. M. and W. Goldsmith (1983). Response of an advanced head-neck model to transient loading. *Journal of Biomechanical Engineering*, **105**, 63–70.
- Winters, J. M. and Stark, L. (1985). Analysis of fundamental human movement patterns through the use of in-depth antagonistic muscle models. *IEEE Transactions on Biomedical Engineering*, **12**, 826–839.
- Winters, J. M. and Stark, L. (1988). Estimated mechanical properties of synergistic muscles involved in movements of a variety of human joints. *Journal of Biomechanics*, **21**, 1027–1041.
- Winters, J., Stark, L. and Seif-Naraghi, A.-H. (1988). An analysis of the sources of musculoskeletal system impedance. *Journal of Biomechanics*, **21**, 1011–1025.
- Winters, J. M. (1990) Hill-based muscle models: a systems engineering perspective. *Multiple Muscle Systems. Biomechanics and Movement Organization*, Edited by J.M. Winters and Woo, S. L.-Y., Springer-Verlag, New York, USA, 69–94.
- Wismans, J. and Spenny, C. H. (1984). *Head-neck response in frontal impacts*. Proc. of the 28th Stapp Car Crash Conference, Chicago, Illinois, USA. Society of Automotive Engineers, 161–171.
- Wismans, J., Van Oorschot, H. and Woltring, H. J. (1986). *Omni-directional human head-neck response*. Proc. of the 30th Stapp Car Crash Conference, San Diego, California, USA. Society of Automotive Engineers, 313–331.
- Wismans, J., Philippens, M., van Oorschot, E., Kallieris, D. and Mattern, R. (1987). *Comparison of human volunteer and cadaver head-neck response in frontal flexion*. Proc. of the 31th Stapp Car Crash Conference, New Orleans, Louisiana, USA. Society of Automotive Engineers, 1–13.
- Wismans, J., Janssen, E. G., Beusenberg, M., Koppens, W. P., and Lupker, H. A. (1994). *Injury Biomechanics*, Eindhoven University of Technology, Faculty of Mechanical Engineering, Eindhoven, The Netherlands.
- Wittek, A. and Kajzer, J. (1995). *A review and analysis of mathematical models of muscle for application in the modelling of musculoskeletal system response to dynamic load*. Proc. of the Ninth Biomechanics Seminar, Edited by C.Högfors and G. Andreasson, Gothenburg. Centre for Biomechanics Chalmers University of Technology and Gothenburg University, 192–216.
- Wolfram, S. (1993). *Mathematica: A System for Doing Mathematics by Computer*. Addison-Wesley Company, New York, USA.

- Yamada, H. (1970). *Strength of Biological Materials*. The Williams & Wilkins Company, Baltimore, USA.
- Yamaguchi, G. T., Sawa, A. G. U., Moran, D. W., Fessler, M. J. and Winters, J. M. (1990). *A survey of human musculotendon actuator parameters*. Multiple Muscle Systems. Biomechanics and Movement Organization, Edited by J.M. Winters and S.L.-Y. Woo, Springer-Verlag, New York, USA, 717–773.
- Zahalak, G. I. (1986). A comparison of the mechanical behavior of the cat soleus muscle with a distribution-moment model. *Journal of Biomechanical Engineering*, **108**, 131–140.
- Zahalak, G. I. and Ma, S. (1990). Muscle activation and contraction: constitutive relations based directly on cross-bridge kinetics. *Journal of Biomechanical Engineering*, **112**, 52–62.